Journal of Medicinal Chemistry Article

J. Med. Chem. **2010,** *53,* 2155–2170 **2155**
DOI: 10.1021/jm901705h

Highly Potent First Examples of Dual Aromatase−Steroid Sulfatase Inhibitors based on a Biphenyl Template[†,‡]

L. W. Lawrence Woo,[§] Toby Jackson,[§] Aurélien Putey,[§] Gyles Cozier,[§] Philip Leonard,[∥,#] K. Ravi Acharya,[∥] Surinder K. Chander,[⊥] Atul Purohit,[⊥] Michael J. Reed,[⊥] and Barry V. L. Potter*[,§]

[§]*Medicinal Chemistry, Department of Pharmacy and Pharmacology and Sterix Ltd, University of Bath, Claverton Down, Bath BA2 7AY, U.K.,* [∥]*Department of Biology and Biochemistry, University of Bath, Claverton Down, Bath BA2 7AY, U.K., and* [⊥]*Endocrinology and Metabolic Medicine and Sterix Ltd, Imperial College London, Faculty of Medicine, St. Mary's Hospital, London W2 1NY, U.K.* [#] *Present address: Biofocus DPI, Chesterford Research Park, Saffron Walden, Essex CB10 1XL, U.K.*

Received November 17, 2009

Single agents against multiple drug targets are of increasing interest. Hormone-dependent breast cancer (HDBC) may be more effectively treated by dual inhibition of aromatase and steroid sulfatase (STS). The aromatase inhibitory pharmacophore was thus introduced into a known biphenyl STS inhibitor to give a series of novel dual aromatase−sulfatase inhibitors (DASIs). Several compounds are good aromatase or STS inhibitors and DASI **20** (IC_{50}: aromatase, 2.0 nM; STS, 35 nM) and its chlorinated congener **23** (IC_{50}: aromatase, 0.5 nM; STS, 5.5 nM) are examples that show exceptional dual potency in JEG-3 cells. Both biphenyls share a *para*-sulfamate-containing ring B and a ring A, which contains a triazol-1-ylmethyl meta to the biphenyl bridge and para to a nitrile. At 1 mg/kg po, **20** and **23** reduced plasma estradiol levels strongly and inhibited liver STS activity potently in vivo. **23** is nonestrogenic and potently inhibits carbonic anhydrase II (IC_{50} 86 nM). A complex was crystallized and its structure was solved by X-ray crystallography. This class of DASI should encourage further development toward multitargeted therapeutic intervention in HDBC.

Introduction

The majority of postmenopausal breast tumors are hormone-dependent and estrogen receptor (ER)-positive. A common therapeutic intervention for this type of cancer is through endocrine therapy. Endocrine agents can act by either diminishing the availability or inhibiting the binding of estrogens to ER. Aromatase catalyzes the conversion of androgens to estrogens in the final step of the biosynthesis of estrogens and is therefore an attractive therapeutic target for inhibition. To this end, a large number of steroidal and nonsteroidal aromatase inhibitors (AIs)[a] have been developed[1−3] and several of them are now in clinical use showing high efficacy against hormone-dependent breast cancers (HDBC).

Most estrogens that originate from the aromatase pathway are stored in the body as steroid sulfates. It is now widely recognized that this reservoir of estrogen sulfates provides an important source of estrogens in tumors when steroid sulfatase (STS) catalyzes the hydrolysis of substrates such as estrone sulfate (E1S) to estrone (E1).[4] Thus, STS has now become an attractive new target for therapeutic intervention. Considerable progress has been made in developing steroidal and nonsteroidal STS inhibitors containing the aryl sulfamate ester moiety, which is the pharmacophore for irreversible inhibition of STS.[4,5] One such compound, **1** (STX64 or BN83495, Figure 1), has become the first STS inhibitor to enter clinical trial for postmenopausal patients with advanced HDBC and has shown encouraging results.[6,7]

Designing hybrid molecules that target multiple biological targets is an emerging and attractive strategy in drug design and discovery.[8] For our application, because of the therapeutic potential of STS inhibitors and the established clinical effectiveness of AIs, it has been reasoned that a concomitant inhibition of aromatase and STS may lead to a more comprehensive estrogen deprivation in patients with HDBC. To this end, we successfully developed three series of single agent dual aromatase and sulfatase inhibitors (DASIs) that are sulfamate derivatives of nonsteroidal AIs 4-((4-bromobenzyl)-[1,2,4]-triazol-4-yl-amino)benzonitrile (e.g., **2**, Figure 1),[9−11] letrozole (e.g., **3**, Figure 1),[12,13] and anastrozole (e.g., **4**, Figure 1).[14] The design of these DASIs shares a common strategy that is to engender the STS inhibitory pharmacophore into an established or experimental AI with minimal structural change incurred to the original scaffold in order to retain and maximize aromatase inhibition.

With the intention of widening further the structural diversity of DASIs, a new design strategy was explored that involves introducing the aromatase inhibitory pharmacophore into a

[†]This article is dedicated to Professor Michael John Reed, B.Sc., M. Sc., Ph.D., D.Sc., FRCPath (1944−2009).

[‡]Protein Data Bank accession code: 2wd3.pdb.

*To whom correspondence should be addressed. Phone: +44 1225 386639. Fax: +44 1225 386114. E-mail: B.V.L.Potter@bath.ac.uk.

[a] Abbreviations: AIs, aromatase inhibitors; DASI, dual aromatase−sulfatase inhibitor; DMA, *N*,*N*-dimethylacetamide; DMPK, drug meta bolism and pharmacokinetics; E1, estrone; E2, estradiol; E1S, estrone sulfate; ER, estrogen receptor; hCAII, human carbonic anhydrase II; HDBC, hormone-dependent breast cancer; NSAIs, nonsteroidal aromatase inhibitors; 2-MeOE2bisMATE, 2-methoxyestradiol-3-*O*,17β-*O*-bissulfamate; PMSG, pregnant mare's serum gonadotropin; STS, steroid sulfatase; STX641, 17β-cyanomethyl-2-methoxyestra-1,3,5(10)-trien-3-*O*-sulfamate; TBAB, tetrabutylammonium bromide.

Published on Web 02/11/2010

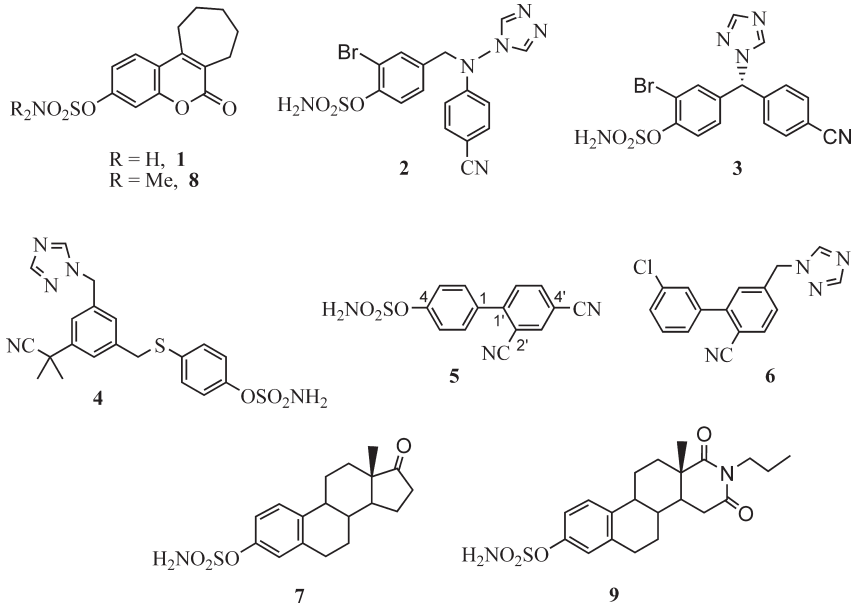

Figure 1. Structures of **1** and its *N*,*N*-dimethylated prodrug **8**, AI 4-((4-bromobenzyl)-[1,2,4]triazol-4-yl-amino)benzonitrile and its DASI derivative **2**, AI letrozole and letrozole-based DASI **3**, AI anastrozole and anastrozole-based DASI **4**, biphenyl STS inhibitor **5**, biphenyl AI **6**, steroidal STS inhibitors **7**, and steroid-like STS inhibitor **9**. X = OSO_2NH_2.

template that has been designed primarily for STS inhibition. While the modification of established STS inhibitors like **1** may be an attractive approach, it was reasoned that the series of biphenyl STS inhibitors reported by Okada et al.[15] represents a more accessible platform for the incorporation of the aromatase inhibitory pharmacophore. One example, **5** (Figure 1), which has two electron withdrawing cyano groups incorporated at the 2′- and 4′-positions and a sulfamate ester at the 4-position, was shown to be a highly potent STS inhibitor.

In a separate development, we also recently exploited the biphenyl motif and successfully designed a new class of nonsteroidal aromatase inhibitors (NSAIs).[16] A particularly potent example is **6** (Figure 1), the IC_{50} value of which against aromatase in JEG-3 cells was found to be 0.22 nM.

Herein, we report a new class of DASI that is based on a biphenyl template. The phenyl ring A of these decorated biphenyls is substituted with a triazol-1-ylmethyl group with or without a second substituent, whereas their phenyl ring B bears a sulfamate group with or without a chlorine atom ortho to it. The in vitro activities of these sulfamoylated compounds, their phenolic precursors, and other derivatives were studied in JEG-3 cells. The extent to which rat liver STS activity is inhibited and plasma estradiol (E2) levels are reduced in vivo by sulfamates **20** and **23** and their respective parent phenols **19** and **22** was determined. A uterine weight gain assay was carried out to assess the estrogenicity of **23**. Because the in vivo sequestration of sulfamate esters by carbonic anhydrase II (hCAII) in red blood cells is thought to enhance the bioavailability and pharmacokinetics of this emerging structural class of drug, the ability of a representative biphenyl derivative **23** to interact with human hCAII was investigated in vitro and an hCAII/23 complex was investigated using X-ray crystallography.

Results and Discussion

Chemistry. A palladium catalyzed Suzuki reaction[17−19] was employed in the preparation of the biphenyl compounds

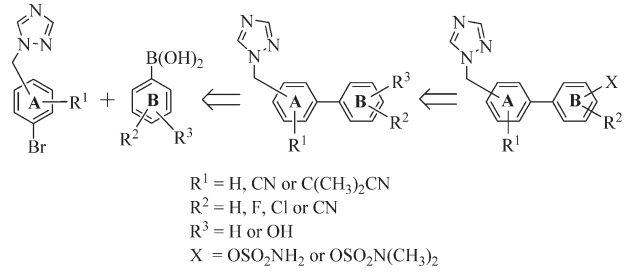

Figure 2. Retrosynthesis of the biphenyl DASIs.

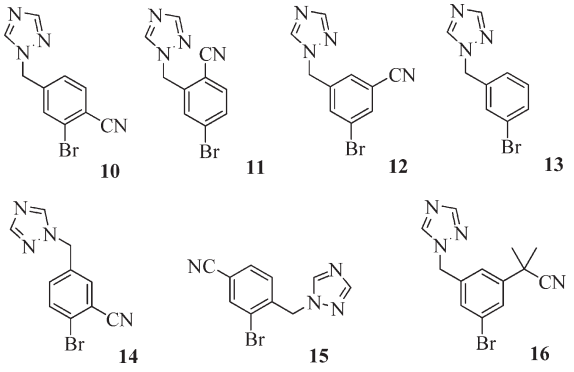

Figure 3. Bromobenzyltriazoles.

where functionalization of the biphenyl scaffold is inherited from already derivatized starting bromobenzyltriazoles and phenylboronic acid (see Figure 2).

We previously described the syntheses of the bromobenzyltriazoles **10**, **11**, and **13**−**16** (Figure 3).[14,16] Likewise, starting material **12** herein (Figure 3) was synthesized by radical bromination of 3-bromo-5-methylbenzonitrile followed by reacting the resulting 3-bromo-5-(bromomethyl)benzonitrile with 1*H*-1,2,4-triazole in the presence of potassium carbonate. 3-Bromo-5-methylbenzonitrile was synthesized in a similar manner as described by Fisher et al.[20] from 2-amino-5-methylbenzoic acid, although the 3-bromo-5-methylbenzoic

Scheme 1[a]

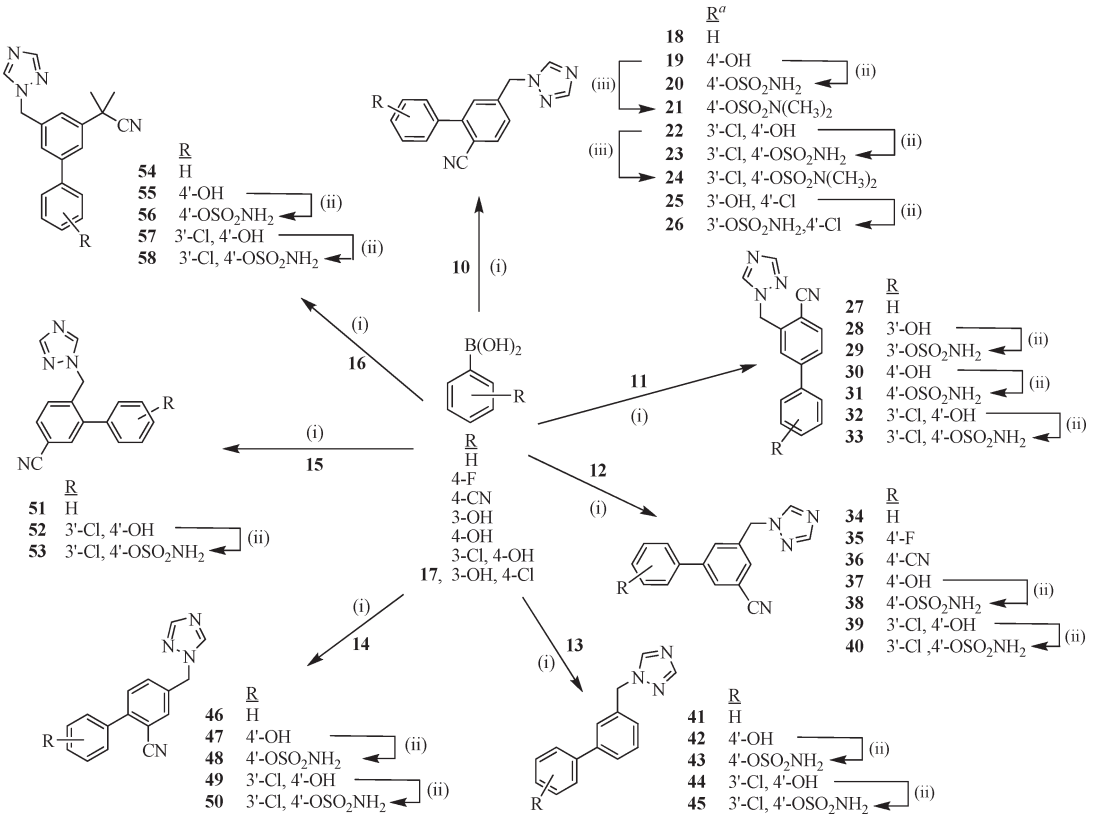

[a] (i) $Pd(OAc)_2$, K_2CO_3, TBAB, H_2O/EtOH, 13−89%; (ii) $ClSO_2NH_2$, DMA, 62−93%; (iii) $ClSO_2N(CH_3)_2$, NEt_3, CH_2Cl_2, 60−90%. Substituents are numbered as shown for presentational uniformity; see Experimental Section for correct numbering of substituents.

acid intermediate was converted to the product 3-bromo-5-methylbenzonitrile in two steps via the 3-bromo-5-methylbenzamide intermediate.

Phenylboronic acid, 4-fluorophenylboronic acid, 4-cyanophenylboronic acid, 3-hydroxyphenylboronic acid, 4-hydroxyphenylboronic acid, and 3-chloro-4-hydroxyphenylboronic acid are all available commercially. 3-Hydroxy-4-chlorophenylboronic acid **17** (Scheme 1) was prepared via lithiation of the commercially available 5-bromo-2-chlorophenol and subsequent treatment with triisopropyl borate.

Several series of biphenyl compounds (**18**−**58**) were prepared (see Scheme 1). The syntheses of the standalone AIs **18**, **27**, **41**, **46**, **51**, and **54** (where R = H) were reported previously,[16] and herein we report the syntheses of congeners **34**−**40**. Sulfamoylated biphenyl compounds were prepared as follows. Corresponding boronic acids and bromobenzyltriazoles were coupled under either convection or microwave initiated palladium catalyzed Suzuki cross-coupling conditions.[21] The resulting phenolic biphenyl precursors (**19**, **22**, **25**, **28**, **30**, **32**, **37**, **39**, **42**, **44**, **47**, **49**, **52**, **55**, and **57**) were then sulfamoylated[22] with sulfamoyl chloride[23] to give **20**, **23**, **26**, **29**, **31**, **33**, **38**, **40**, **43**, **45**, **48**, **50**, **53**, **56**, and **58**. The *N*,*N*-dimethylsulfamates **21** and **24** were prepared by reaction of the phenols **19** and **22** with *N*,*N*-dimethylsulfamoyl chloride in dichloromethane in the presence of base.

Inhibition of Aromatase and Steroid Sulfatase in Vitro by Sulfamoylated Compounds. The in vitro inhibitory activities of sulfamoylated compounds against aromatase and STS in JEG-3 cells are shown in Table 1. The various structural subclasses of inhibitors have been broken down into groups I−VII. As references, the clinical AIs anastrozole[14] and letrozole,[12] the investigational STS inhibitor **1** (Figure 1), and the biphenyl STS inhibitor **5** (Figure 1) were studied in the same assay. Although the STS inhibitory potential of anastrozole and letrozole was not investigated here, they are expected to be ineffective against STS and act primarily as AIs. Compound **1** has an IC_{50} value of 1.5 nM against STS but shows relatively insignificant aromatase inhibition. The biphenyl **5** inhibits STS strongly, albeit being more than 10-fold less active than **1**. As anticipated, there was no significant aromatase inhibition shown by **5**. Therefore, all these reference compounds are acting individually either as AIs or STS inhibitors but not as DASIs in JEG-3 cells.

Compounds **20**, **21**, **23**, **24**, and **26** of structural group I have in common a cyano group on phenyl ring A ortho to the biphenyl bridge and para to the triazol-1-ylmethyl moiety. The simplest derivative in this series is **20**, which has a sulfamate group on phenyl ring B at the 4′-position. This compound inhibits aromatase and STS with IC_{50} values of 2 and 35 nM, respectively. It is interesting to note that the STS inhibitory potency of **20** is of the same order of magnitude as **5**, perhaps reflecting in part the similar pK_a values of their parent phenols (9.32 and 9.08 as calculated by ACD/Laboratories Software v 8.14 for **19** and 4′-hydroxy-2,4-biphenyldicarbonitrile, respectively). The introduction of a chlorine atom ortho to the sulfamate group and at the 3′-position of **20** renders a marked improvement on the inhibitory activities of the resulting compound **23**, the IC_{50} values of which against aromatase and STS are 0.5 and 5.5 nM, respectively. Hence, in JEG-3 cells, **23** is 4-fold and 6-fold better than **20** in inhibiting aromatase and STS, respectively, is equipotent to letrozole as an AI and inhibits STS in the

Table 1. In Vitro Inhibition of Aromatase and STS Activity in JEG-3 Cells by Anastrozole, Letrozole, **1**, **5**, and Sulfamoylated Compounds **20**, **21**, **23**, **24**, **26**, **29**, **31**, **33**, **38**, **40**, **43**, **45**, **48**, **50**, **53**, **56**, and **58**

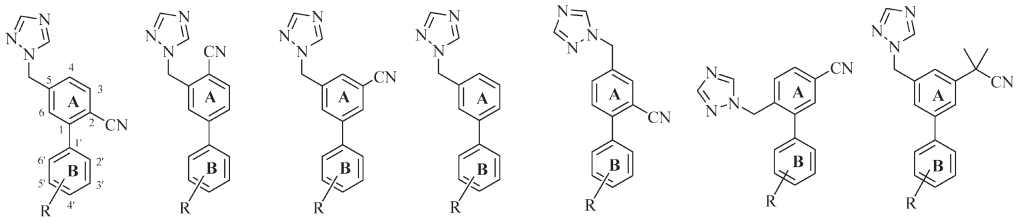

structural group	compd	R[a]	aromatase IC_{50} (nM) or % inhibition @ 1 μM	STS IC_{50} (nM) or % inhibition @ 10 μM
−	anastrozole	−	1.5 ± 0.5	nd
−	letrozole	−	0.89 ± 0.13	nd
−	**1**	−	300 ± 42	1.5 ± 0.3
−	**5**	−	47 ± 3.7%[b]	16.3 ± 2
I	**20**	4′-OSO_2NH_2	2.0 ± 0.20	35.0 ± 5.0
	21	4′-$OSO_2N(CH_3)_2$	0.50 ± 0.05	> 10000
	23	3′-Cl, 4′-OSO_2NH_2	0.50 ± 0.01	5.50 ± 0.5
	24	3′-Cl, 4′-$OSO_2N(CH_3)_2$	2.40 ± 1.0	> 10000
	26	3′-OSO_2NH_2, 4′-Cl	0.35 ± 0.07	> 10000
II	**29**	3′-OSO_2NH_2	63.4 ± 2.1%	> 10000
	31	4′-OSO_2NH_2	176 ± 25	140 ± 10
	33	3′-Cl, 4′-OSO_2NH_2	146 ± 11	32.6 ± 6.3
III	**38**	4′-OSO_2NH_2	280 ± 10	> 10,000
	40	3′-Cl, 4′-OSO_2NH_2	80 ± 18	6333 ± 577
IV	**43**	4′-OSO_2NH_2	275 ± 6	5500 ± 300
	45	3′-Cl, 4′-OSO_2NH_2	70 ± 5	160 ± 10
V	**48**	4′-OSO_2NH_2	284 ± 26	28.6 ± 2.0
	50	3′-Cl, 4′-OSO_2NH_2	571 ± 53	29 ± 2.0
VI	**53**	3′-Cl, 4′-OSO_2NH_2	1.90 ± 0.06	> 10000
VII	**56**	4′-OSO2NH_2	17.5 ± 2.0	> 10000
	58	3′-Cl, 4′-OSO_2NH_2	0.3 ± 0.1	68.2 ± 1.6%

[a] Substituents are numbered as shown for presentational uniformity; see Experimental Section for correct numbering of substituents. [b] Inhibition @ 10 μM, −: not applicable, nd: not determined.

same order of magnitude as **1**. On the basis of past observations,[9−11] the higher aromatase inhibition observed for **23** compared to **20** can be attributed to the increase in the lipophilicity of **23** conferred by its chlorine atom. We have demonstrated in previous work, within limits, that a general inverse relationship exists between the STS inhibitory potency of a sulfamate and the pK_a value of its corresponding parent phenol.[4,5,24,25] Given that the pK_a value of **22** is 7.89 (calculated according to ACD/Laboratories Software v 8.14), which is significantly lower than that of **19** (9.32), the increase in STS inhibition observed for **23** compared with **20** could be rationalized by the presence of the chlorine atom ortho to its sulfamate group. The electron-withdrawing effect of the halogen increases the leaving group ability of the parent phenol **22,** which in return facilitates the sulfamoylation and hence inactivation of the enzyme by the sulfamate group of **23**. While the electron-withdrawing cyano groups of **5** are both conjugated to its sulfamate group and are hence conducive to the reduction of the pK_a of its parent phenol (4′-hydroxybiphenyl-2,4-dicarbonitrile), the presence of a chlorine atom at the 3′- and a cyano group at the 2-position of the biphenyl system confers a more marked reduction in the pK_a value of the phenol **22**. This factor may help in part to explain why **23** is a stronger STS inhibitor than **5**. A recent study with *Pseudomonas aeruginosa* arylsulfatase has shown that the stoichiometry of inactivation by 1 has a value of around 3, with one interpretation being that the inactivation process of this arylsulfatase could involve multiple sulfamoylation events.[26] Although no similar experiment has yet been carried out with STS, it is possible that the inhibition of STS elicited by **23** may also involve more than just one single sulfamoylation event or, perhaps more likely, proceed by a complex process.

When the positions of the chlorine atom and the sulfamate group in **23** are transposed, the resulting compound **26** shows a slight increase in aromatase inhibition but a substantial reduction in STS inhibition. A similar finding was made in the series of DASIs, which are derivatives of AI 4-((4-bromobenzyl)-[1,2,4]triazol-4-yl-amino)benzonitrile.[10] It was observed that substituted or unsubstituted *meta*-sulfamate

derivatives are stronger AIs but much weaker STS inhibitors than their *para*-sulfamate counterparts.

The *N*,*N*-dimethylation of the sulfamate group of **20** to give **21** improves aromatase inhibition by 4-fold (IC_{50} for **21** = 0.5 nM, cf. 2 nM for **20**). In contrast, the same dimethylation of the sulfamate group of **23** to give **24** reduces aromatase inhibition by nearly 5-fold. It is not clear why the effects of *N*,*N*-dimethylation of **20** and **23** are so disparate despite both **21** and **24** being more lipophilic than their nonmethylated counterparts. In general, an increase in the lipophilicity of an inhibitor normally benefits aromatase inhibition. For STS inhibition, the very weak activities observed for **21** and **24** are anticipated. It has been shown that the *N*-piperidino- and *N*,*N*-dibenzyl derivatives of estrone 3-*O*-sulfamate (**7**, Figure 1) are significantly weaker STS inhibitors than **7** in vitro, although the *N*-acetyl derivative, which has one free proton on the sulfamate nitrogen atom, shows moderate irreversible STS inhibition.[27] Similarly, when the sulfamate group of the clinical agent **1** (Figure 1) was *N*,*N*-dimethylated, the resulting derivative **8** (Figure 1) was shown to be inactive against STS in vitro.[28] These findings clearly suggest that a ligand is to have a fully unsubstituted sulfamate group, i.e., H_2NSO_2O-Ar, in order to maximize active site-directed irreversible STS inhibition in vitro. However, like **1**, **8** at 1 and 10 mg/kg doses inhibits almost completely mouse liver and skin STS activities 24 h after oral administration of the compound.[29] There is evidence to suggest that **8** is a pro-drug of **1** that is metabolized in vivo and undergoes *N*,*N*-demethylation to give **1** that subsequently inhibits STS in treated animals. By the same token, it is entirely possible that **21** and **24**, although inactive as STS inhibitors in vitro, are indeed pro-drugs of **20** and **23**, respectively, and hence can be demethylated and become active against STS in vivo. More studies are required to explore this potential property of **21** and **24**.

While keeping the triazol-1-ylmethyl moiety meta to the biphenyl bridge, the effects on biological activities of relocating the cyano group of **20** and **23** to other positions on phenyl ring A or removing it entirely were explored. Compounds **29**, **31**, and **33** (structural group II) have a cyano group ortho to a triazol-1-ylmethyl moiety but para to the biphenyl bridge, whereas compounds **38** and **40** (structural group III) have a cyano group meta to both the biphenyl bridge and the triazol-1-ylmethyl moiety. Compounds **43** and **45** (structural group IV) have no cyano group on phenyl ring A apart from a triazol-1-ylmethyl moiety meta to the biphenyl bridge. As shown in Table 1, these derivatives are relatively much weaker AIs. Apart from **33** of group II, the introduction of a chlorine atom ortho to the sulfamate group significantly improves the aromatase inhibitory potency of **40** (group III) and **45** (group IV) over their respective nonchlorinated counterparts **38** and **43**. However, despite **40** and **45** being the two most active AIs in structural groups II−IV, their activities are at least 2 orders of magnitude lower than those of their congeners **20**, **23**, and **26** in group I. These results clearly demonstrate the importance of having a triazol-1-ylmethyl moiety meta to the biphenyl bridge and para to the cyano group on phenyl ring A for high aromatase inhibitory potency to be maintained. Any relocation or removal of the cyano group is detrimental to biological activity. Compound **29**, which has a 3′-sulfamate, is a much weaker AI than the 4′-sulfamate derivative **31**, although the relocation of the sulfamate group in a similar fashion from the 4′-position of **23** to the 3′-position of **26** results in a small beneficial effect.

The STS inhibitory activities of sulfamates in structural groups II−IV are significantly weaker than those of derivatives from group I. The best STS inhibitor out of these groups is **33** (IC_{50} = 32.6 nM) that has the electron-withdrawing cyano group and the chlorine atom both conjugated to the sulfamate group.

On keeping the cyano group ortho to the biphenyl bridge and moving the triazol-1-ylmethyl moiety from the 3- to the 4-position of phenyl ring A where it is meta to the cyano group and para to the biphenyl bridge, the resulting structural group V derivatives **48** and **50** remain relatively weak AIs (IC_{50} = 284 and 571 nM, respectively). Although both these two sulfamates have a cyano group ortho to the biphenyl bridge, the substantial reduction in their inhibitory activities observed compared to **20** and **23** further demonstrate the importance of having a para relationship between the triazol-1-ylmethyl moiety and the cyano group for potent aromatase inhibition. Interestingly, the STS inhibitory activities of **48** and **50** are comparable to that of **20**, with IC_{50} values at around 30 nM. However, it is not clear why in this structural class the chlorine atom of **50** does not confer as anticipated an additional advantage over its nonchlorinated congener **48** on STS inhibition. Nonetheless, for **48** and **50** as well as other relatively more active STS inhibitors identified in this work, i.e., **20**, **23**, **31**, **33**, and **45**, they all share a common feature, which is the conjugation of the cyano group and/or the chlorine atom to the sulfamate group.

To further investigate the para relationship between the triazol-1-ylmethyl moiety and the cyano group on phenyl ring A, the two functionalities were placed respectively ortho to and meta to the biphenyl bridge to give **53** (structural group VI). As shown in Table 1, **53** (IC_{50} = 1.9 nM) is equipotent to **20** (IC_{50} = 2.0 nM) but some 4-fold weaker than **23** (IC_{50} = 0.5 nM) as an AI. In conjunction with the SAR obtained so far, this finding further confirms the importance of having a para relationship between the triazol-1-ylmethyl moiety and the cyano group on phenyl ring A for this structural class of biphenyl-based DASIs. However, for optimal aromatase inhibition, it requires the heme ligating triazol-1-ylmethyl moiety to be meta to and the cyano group ortho to the biphenyl bridge, which is a feature of those compounds in structural group I. In contrast to their similar abilities in inhibiting aromatase, compounds **20**, **23**, and **53** inhibit STS quite differently. While **20** and **23** are inhibitors of STS with nanomolar IC_{50} values, the inhibition of STS by **53** remains ineffective at micromolar concentrations.

In our recent work, it was observed that DASIs could be designed by replacing one of the anastrozole 2-methylpropanenitrile groups with linkers attached to an aryl sulfamate, i.e., the STS pharmacophore for irreversible inhibition.[14] Herein, we replace one of the side-arms of anastrozole directly with a phenyl sulfamate to give the biphenyl derivatives **56** and **58** (structural group VII). These two compounds are related to **20** and **23** structurally except they have no cyano group ortho to the biphenyl bridge but instead a 2-methylpropanenitrile group meta to it. As shown in Table 1, while **56** is a moderate to good AI, its chlorinated congener **58** is exceptionally potent; the IC_{50} value (0.3 nM) is comparable to those of top AIs discovered in this work (i.e., **21**, **23**, and **26**). On comparing **56** and **58** with **38** and **40** from structural group III, the replacement of the cyano group with a 2-methylpropanenitrile group at the 3-position of phenyl

Table 2. In Vitro Inhibition of Aromatase Activity in JEG-3 Cells by Anastrozole, Letrozole, and Nonsulfamoylated Compounds **18**, **19**, **22**, **25**, **27**, **28**, **30**, **32**, **34**−**37**, **39**, **41**, **42**, **46**, **47**, **49**, **51**, **52**, **54**, **55**, and **57**

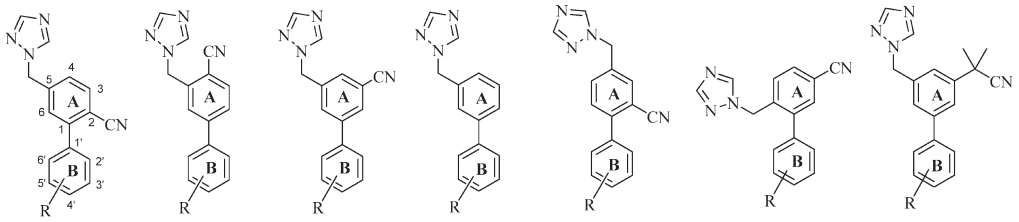

structural group	compd	R[a]	aromatase IC_{50} (nM) or % inhibition @ 1 μM
−	anastrozole	−	1.5 ± 0.5
−	letrozole	−	0.89 ± 0.13
I	**18**	H	0.20 ± 0.02[b]
	19	4′-OH	0.20 ± 0.01
	22	3′-Cl, 4′-OH	0.15 ± 0.03
	25	3′-OH, 4′-Cl	0.22 ± 0.01
II	**27**	H	68.8 ± 1.4%[b,c]
	28	3′-OH	14.4 ± 1.4
	30	4′-OH	76.4 ± 2.4%[d]
	32	3′-Cl, 4′-OH	74.0 ± 12
III	**34**	H	29.3 ± 2.4
	35	4′-F	19 ± 1
	36	4′-CN	52 ± 3
	37	4′-OH	112 ± 10
	39	3′-Cl, 4′-OH	24 ± 1
IV	**41**	H	210 ± 30[b]
	42	4′-OH	79.0 ± 1.9%[e]
	44	3′-Cl, 4′-OH	85.3 ± 1.2%[f]
V	**46**	H	4.6 ± 1.2[b]
	47	4′-OH	920 ± 121
	49	3′-Cl, 4′-OH	380 ± 190
VI	**51**	H	1.7 ± 0.8[b]
	52	3′-Cl, 4′-OH	0.800 ± 0.03
VII	**54**	H	0.50 ± 0.10[b]
	55	4′-OH	6.0 ± 1.0
	57	3′-Cl, 4′-OH	0.1 ± 0.1

[a] Substituents are numbered as shown for presentational uniformity; see Experimental Section for correct numbering of substituents. [b] Data from ref 16; −: not applicable. [c] 23.9 ± 2.9% @ 0.1 μM. [d] 35.1 ± 6.0% @ 0.1 μM. [e] 24.6 ± 7.0% @ 0.1 μM. [f] 36.6 ± 2.2% @ 0.1 μM.

ring A enhances aromatase inhibition significantly. Previous molecular modeling studies carried out on the nonsulfamoylated congener **54** (R = H, Scheme 1 and Table 2) has suggested that its 2-methylpropanenitrile group might form a H-bond with Ser478 of the aromatase active site.[16] It is possible that, inter alia, a similar favorable interaction with the aromatase enzyme active site also operates in **38** and **40**. Compounds **38** and **40** are very weak inhibitors of STS in JEG-3 cells. Their lack of in vitro activity against STS can be attributed to a combination of unfavorable steric and electronic factors, as postulated for the structurally related anastrozole-based DASIs.[14]

Inhibition of Aromatase in Vitro by Nonsulfamoylated Compounds. According to the various mechanisms of action proposed by our group,[4,5,23,24] the immediate product released after the irreversible inactivation of STS by a sulfamate-based STS inhibitor is expected to be its corresponding phenol, although the quantity released by this route in vivo is considered restricted once all the STS activity has been inactivated.[30] However, given the chemical stability issues observed for some aryl sulfamates, it is reasonable to expect the formation of the parent phenol could in principle continue as a result of gradual hydrolytic cleavage of the sulfamate group of any ligand that presents in the plasma over time. For this reason and also because they possess the pharmacophore for aromatase inhibition, the parent phenols of sulfamates and also the new compounds **34**−**36** were assayed for aromatase inhibition in JEG-3 cells (Table 2). Anastrozole and letrozole were used as reference AIs, and the IC_{50} values for the unsubstituted derivatives (**18**, **27**, **41**, **46**, **51**, and **54**) reported previously[16] are included for comparison.

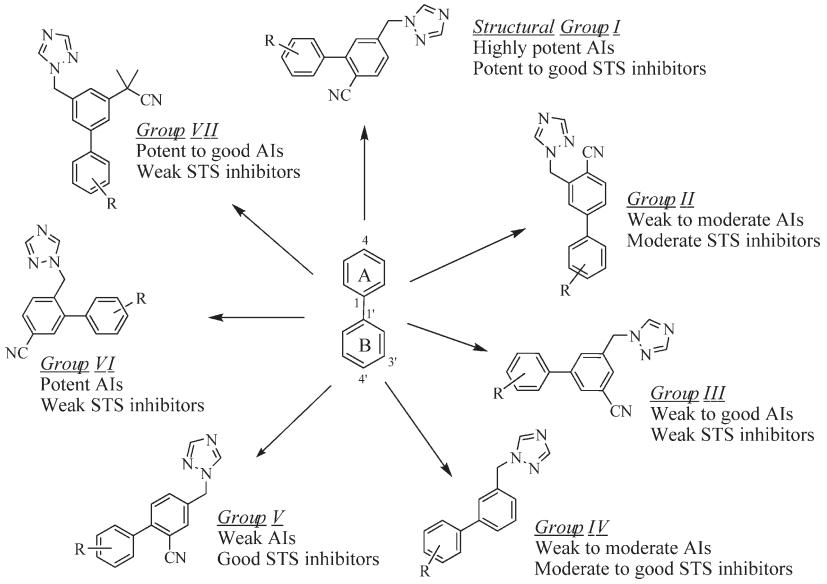

Figure 4. Generalized summary of the SAR for aromatase and STS inhibition in JEG-3 cells by biphenyl-based DASIs and their parent phenols (R = 4′-OH; 4′-OH, 3′-Cl; 4′-OSO_2NH_2; 4′-OSO_2NH_2, 3′-Cl).

As shown in Table 2, the parent phenol of most structural groups is in general a stronger AI than its corresponding sulfamate. This observation is expected because a similar profile was observed for the parent phenols from other classes of DASIs. Of the phenols tested, **19**, **22**, and **25** (structural group I: 5-triazolylmethyl and 2-cyano), **52** (group VI: 6-triazolylmethyl and 3-cyano), and **55** and **57** (group VII: 5-triazolylmethyl and 3-(2-methylpropanenitrile)) were found to inhibit aromatase most strongly. Their IC_{50} values are comparable to or within an order of magnitude of those observed for anastrozole and letrozole. Interestingly, although not comparable in terms of the level of potency, the three most potent groups of AIs within the series of nonhydroxylated biphenyl-based AIs studied by Jackson et al.[16] also belong to these three structural groups. Hence, it appears that these biphenyl templates and their substituents concertedly bind well to the aromatase active site and interact favorably with the heme and certain neighboring amino acid residues. The fact that the respective parent phenols, **19** (IC_{50} = 0.2 nM) and **22** (IC_{50} = 0.15 nM), of the two most active DASIs **20** and **23** are themselves even more potent AIs suggest that they should in their own right further inhibit aromatase, and do so potently, on release either chemically or after STS inhibition.

Of phenols belonging to the structural groups II−V, the hitherto unexplored compounds **34**−**37** and **39** of structural group III, whose triazol-1-ylmethyl moiety and cyano group are both meta to the biphenyl bridge, turn out to be the more potent AIs. However, the phenols from groups I, VI, and VII phenols are clearly much more potent AIs whose aromatase IC_{50} values are between 2 and 3 orders of magnitude lower than those observed for phenols from structural groups II−V.

In summary, for inhibition of individual enzymes, compounds primarily from structural groups VI and VII are good to potent aromatase inhibitors, whereas some examples from group II, IV, and V show moderate to good STS inhibition. However, for dual inhibition of aromatase and STS, the best two DASIs in this work are **20** (IC_{50}Arom = 2.0 nM and IC_{50}STS = 35 nM) and **23** (IC_{50}Arom = 0.5 nM and IC_{50}STS = 5.5 nM) from structural group I, whose triazol-1-ylmethyl moiety on phenyl ring A is meta to the biphenyl bridge and para to the cyano group. Both of their sulfamate groups are para to the biphenyl bridge on phenyl ring B, but **23** has an additional chlorine atom ortho to its sulfamate group. In general, parent phenols of DASIs are better AIs and those from structural groups I, VI, and VII are exceptionally potent. A generalized summary of the key SAR for dual aromatase and STS inhibition by *para*-sulfamoylated biphenyl-based DASIs and their parent phenols is shown in Figure 4.

Table 3. The Effects of **19**, **20**, **22**,and **23**, Letrozole (an AI) and **9** (an STS Inhibitor) on PMSG-Induced Plasma E2 Concentrations (Aromatase Activity) and Liver STS Activity in the Immature Rat 3 h after Oral Dosing

treatment[a]	plasma E2 levels (pg/mL)	aromatase inhibition (%)[b]	STS inhibition (%)
control	17 ± 3	95 ± 1	0 ± 8
PMSG	334 ± 85	0 ± 26	16 ± 6
letrozole	49 ± 11	85 ± 3	0 ± 10
19	94 ± 33	72 ± 10	10 ± 7
20	124 ± 74	63 ± 22	77 ± 12
22	297 ± 90	11 ± 27	5 ± 22
23	132 ± 22	60 ± 7	92 ± 6
9	nd	nd	99 ± 0.1

[a] Dose: letrozole, 0.1 mg/kg; others, 1 mg/kg. [b] Results are expressed as the percentage inhibition of PMSG stimulated E2 levels. The statistical significance for aromatase and STS activities in control and treated groups (n = 3) was assessed using Student's t test. nd: not determined.

Inhibition of Aromatase and Sulfatase in Vivo. Compounds **19**, **20**, **22**, **23**, letrozole, and **9** (Figure 1, a highly potent steroid-like STS inhibitor[31−33]) were studied in vivo (Table 3). Immature female Wistar rats (20 days), pretreated with 200 IU/0.1 mL sc of PMSG (pregnant mare's serum gonadotropin), were treated 3 days later with individual agent at a 1 mg/kg po dose (letrozole, 0.1 mg/kg po). Plasma E2 levels and liver STS activity were determined 3 h after dosing.

The phenol **19** inhibits aromatase strongly and reduces E2 plasma levels by 72% compared with those of rats pretreated with PMSG (Table 3). In contrast and unexpectedly, the phenol **22** failed to reduce plasma E2 levels significantly.

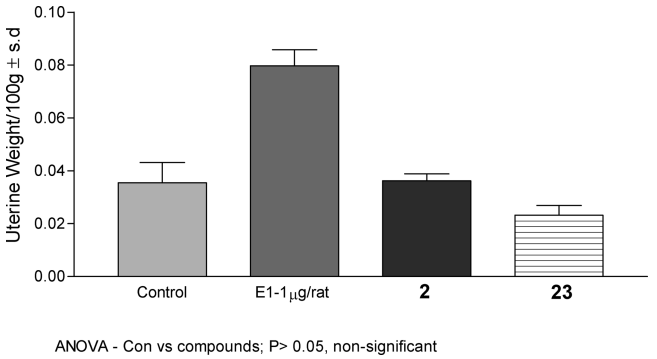

Figure 5. The effect on uterine growth in the ovariectomized rat after an oral dosing of **2** and **23** at 10 mg/kg for 4 days. Mean ± SD of triplicate measurements. ANOVA: control vs compounds; $P > 0.05$, nonsignificant.

Given the high aromatase inhibitory potency of **22** in vitro (IC_{50} = 0.15 nM, Table 2), it is possible that its weak aromatase inhibition observed in vivo could be related to a poor oral bioavailability or drug delivery of **22**. In the absence of a sulfamate group, **19** predictably has negligible inhibitory effect on liver STS activity (Table 3). Putting aside the potential DMPK issue postulated for **22**, this compound is not expected to be active against STS for the same reason because it lacks a sulfamate group. DASIs **20** and **23** inhibit aromatase strongly, rendering a reduction in E2 plasma levels by 63% and 60%, respectively, albeit not as potent as letrozole (85%) at 0.1 mg/kg po. Although the aromatase IC_{50} value for **23** is 4-fold lower than that of **20** in JEG-3 cells (Table 1), **20** and **23** apparently show similar inhibitory activities in vivo. Both DASIs inhibit liver STS activity potently but to a different extent with 75% and 92% inhibition observed for **20** and **23**, respectively. In vitro, DASI **23** is some 6-fold more potent than **20** as an STS inhibitor (Table 1). In the same assay, **9** inhibits liver STS activity almost completely. These results clearly demonstrate the significant dual inhibition of aromatase and STS exhibited by **20** and **23** in vivo on oral administration.

Estrogenicity. It would be undesirable for an antiendocrine agent to possess any endocrinological effect(s) that it is designed to counteract. Hence, only a nonestrogenic DASI will be of suitable use in endocrine therapy for HDBC. With the exception of **18**, **25**−**29**, **34**, **41**, **46**, **51**, and **54** (Scheme 1), other compounds studied in this work share a common 4-hydroxybiphenyl template. It has been shown in the literature that compounds which bear this template and are structurally similar to E2 can possess estrogenic activity.[34,35] Given that the immediate product or metabolite released upon either STS inhibition or by gradual chemical degradation of a biphenyl sulfamate is its parent phenol (vide supra), DASI **23** was therefore selected and tested for estrogenicity in vivo. Using adult ovariectomized rats, **23** was administered in a 10 mg/kg po dose daily for 4 days, after which time the rats were weighed, sacrificed, and uteri removed for weighing. As shown in Figure 5, **23** is not estrogenic as there was no increase in uterine weight observed in treated animals. Similarly, DASI **2** (Figure 1) was also found to be nonestrogenic. This result, in conjunction with the report that the biphenyl STS inhibitor **5** (Figure 1) is also nonestrogenic in vivo,[15] suggests the substituted biphenyl template adopted in this work for the design of DASIs may not be intrinsically pro-estrogenic.

Table 4. IC_{50} Values for the Inhibition of hCAII by **7** and **23** from Initial Rate Experiments Performed in Triplicate

compd	hCAII IC_{50} (nM)
7	56 ± 10
23	86 ± 8

Interactions with hCAII. Like sulfonamides, sulfamate esters also reversibly inhibit hCAII. In its monoanionic form, the sulfamate moiety (OSO_2NH^-) coordinates to the zinc ion of the active site. Many aryl sulfamates have been shown to inhibit hCAII in vitro.[28,36−39] Given that **23** represents a new structural class of highly potent DASI, the potential of **23** to inhibit hCAII in vitro was assessed alongside **7** (Figure 1) as reference, which is a known potent hCAII inhibitor.

As shown in Table 4, DASI **23** inhibits hCAII potently with an IC_{50} value in the same order of magnitude as **7**. This result demonstrates the potential of **23** to be sequestrated into hCAII in erythrocytes, which is an important mechanism for optimizing oral activity, pharmacokinetics, and protecting against first pass metabolism as shown with **1**.[40]

Several X-ray crystal structures of sulfamate-based compounds bound to hCAII have been reported recently. These include steroid sulfatase inhibitors **1**,[41] **7**,[37] and 3-sulfamoyloxy-*N*-(3′-pyridin-1′-ylmethyl)-16,17-*seco*-estra-1,3,5(10)-triene-16,17-imide,[33] two examples of a DASI,[42] 2-MeOE2bisMATE, a multitargeted antitumor agent,[38] and a related agent STX641.[39] With the excellent potency shown by **23** against hCAII, we explored the co-crystallization of **23** with the enzyme and now report the interaction of this compound with hCAII using protein crystallography (Figure 6).

Co-crystallization of hCAII with **23** produced crystals of the enzyme−inhibitor complex in the $P2_1$ space group. During the early stages of refinement, the presence in the binding site of the active site zinc(II) atom and **23** was identified by strong positive density in the $|F_o| - |F_c|$ map corresponding to the sulfamate group of **23** within 2.5 Å of the active site zinc(II) atom. The final model (Figure 6A) was produced by addition of the inhibitor molecule, Zn(II) atom, and water molecules, with manual rebuilding and further refinement using CCP4i[45] and Coot,[46] giving final R_{free} and R_{cryst} values of 0.19 and 0.15 respectively.

DASI **23** was refined with an occupancy of 0.8, and there was almost complete density for each part of the molecule in the final model (Figure 6B). The interactions involving the sulfamate group of **23**, the active site Zn(II) atom and the histidine triad (His94, His96, and His119), as well as the residues at the bottom of the active site funnel, are similar to those observed in previous structures of the enzyme with sulfamate containing inhibitors.[33,37,41] The biphenyl moiety of **23** is located coming out of the center of the active site funnel. Many hCAII inhibitors, including **1**,[41] **7**,[37] and a steroid-like STS inhibitor,[33] have a significant degree of interaction with hydrophobic residues lining the funnel. In contrast, **23** bound more toward the center of the funnel, only Val121, Phe131, and Leu198 are close enough to the biphenyl skeleton to form productive hydrophobic interactions (Figure 6B).

With there only being a few of these hydrophobic interactions, the binding of **23** to hCAII could be bolstered through the triazole ring being orientated toward a small hydrophilic cleft situated close to the entrance of the active site funnel which is flanked by Leu60, Asn62, Glu69, and Glu238 (Figure 6B). There are two possible orientations of

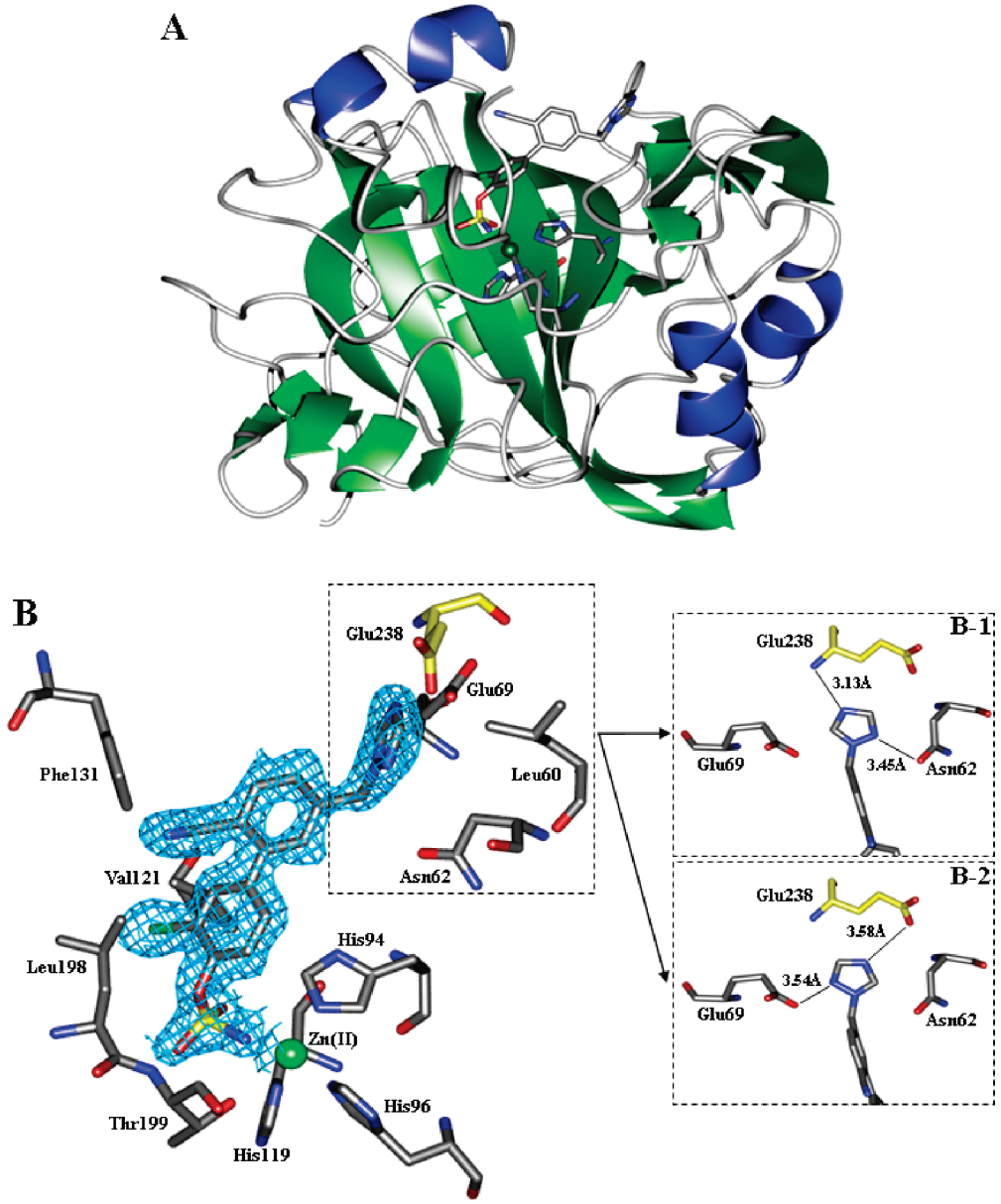

Figure 6. (A) Ribbon diagram showing the overall structure of the hCAII−**23** complex. Secondary structure α-helices are shown in blue and β-sheets in green. The inhibitor molecule, residues His94, His96, and His119 are shown as sticks, and the zinc ion is shown in dark green. (B) Diagram of the active site region in the hCAII−**23** complex. Only residues with interactions to **23** or the active site zinc are shown for clarity. Glu238 from the symmetry related molecule is shown in yellow. Density for the $2|F_o| - |F_c|$ map (light blue) contoured at 1.0σ is shown for **23**. (B-1 and B-2) Close up views of the two possible triazole orientations are shown, with only the residues that could hydrogen bond to the triazole shown for clarity. Black lines link atoms capable of hydrogen bonding and the distances between these atoms are shown. This diagram was prepared using CCP4 mg[43] and POV-Ray.[44]

the triazole ring in this cleft, where the difference between these two orientations involves a 180° rotation of the ring. In one orientation (Figure 6B-1), the 2-*N* of the triazole ring would be 3.45 Å from Asn62, and the 4-*N* of the triazole being 3.13 Å from the backbone nitrogen of Glu238 from a symmetry related molecule. In the second orientation (Figure 6B-2), the 2-*N* of the triazole ring is 3.54 Å from Glu69, and the 4-*N* of the triazole is 3.58 Å from the side-chain oxygen of Glu238 from a symmetry related molecule. These distances are all too long for optimal hydrogen bonding. From the electron density of **23**, it is not possible to conclude which orientation is adopted, or whether it is a mixture of the two orientations, but the orientation shown in Figure 6B-1 does have the shorter distances, in particular the 3.13 Å distance between the triazole and the symmetry related Glu238, and therefore may be the predominant orientation in the crystal structure. It is also worth noting that in solution there would be no symmetry molecule; therefore there is only the possibility of one hydrogen bond from either Asn62 or Glu69 that could anchor the triazole in this cleft. During the refinement of the structure of hCAII in complex with **23**, density for a second inhibitor molecule was observed in the $2|F_o| - |F_c|$ map contoured at 1.0σ. This was in a similar location to the second inhibitor binding site observed in the structure of hCAII/2-MeOE2bisMATE complex.[38] Thus, in summary, the potent inhibition of hCAII observed for **23** can be attributed to the anchoring of the ligand at both ends to the binding site of the protein,

bolstered by additional hydrophobic interactions of its biphenyl ring with some neighboring amino acid residues. It seems likely that this hCAII interaction will also engender good in vivo properties for this new class of dual inhibitor.

Conclusions

By introducing the aromatase inhibitory pharmacophore into the biphenyl STS inhibitor **5**, a series of biphenyl-based DASIs was designed and synthesized. The phenyl ring A of these biphenyls is substituted with a triazol-1-ylmethyl group with or without a second substituent, whereas phenyl ring B bears a sulfamate group with or without a chlorine atom ortho to it. SAR studies derived from seven structural groups have shown that while individual good to potent AIs or moderate to good STS inhibitors are obtained, potent DASIs are realized primarily from structural group I, where the *para*-sulfamate containing phenyl ring B is coupled with phenyl ring A which contains a triazol-1-ylmethyl moiety meta to the biphenyl bridge and para to the cyano group. The best two DASIs in this work are **20** (IC_{50}Arom = 2.0 nM and IC_{50}STS = 35 nM) and its chlorinated congener **23** (IC_{50}Arom = 0.5 nM and IC_{50}STS = 5.5 nM). As expected, the parent phenols of sulfamoylated compounds including **20** and **23** are generally even stronger AIs, with those from structural groups I, VI, and VII exceptionally potent. The *N*,*N*-dimethylsulfamate derivatives of **20** and **23** are potent AIs but inactive as STS inhibitors in JEG-3 cells. On oral administration of **20** and **23** at 1 mg/kg to immature female Wistar rats 3 days after pretreating them with PMSG, both compounds inhibit aromatase strongly 3 h after dosing, rendering a reduction in E2 plasma levels by 63% and 60%, respectively, albeit not as potent as letrozole (85%) at 0.1 mg/kg po. From the same experiment, **20** and **23** were found to inhibit liver STS activity by 75% and 92%, while **9**, the potent steroid-like STS inhibitor, inhibits liver STS activity almost completely. At an oral dose of 10 mg/kg given for 4 days, DASI **23** was found to be nonestrogenic, as shown by the lack of uterine growth observed in treated ovariectomized rat. Like other sulfamoylated compounds reported in the literature, **23** inhibits hCAII potently. The structure of a complex of **23** with hCAII was solved through X-ray crystallography. In summary, a new class of biphenyl-based DASIs has been discovered. The two best compounds **20** and **23** are highly potent against aromatase and STS in JEG-3 cells and show strong dual inhibitory activity in vivo on oral administration. Compound **23**, in addition, is nonestrogenic and shows potential for sequestration into hCAII in erythrocytes, which influences its in vivo behavior. All these results suggest that biphenyl-based DASIs like **20** and **23** can be further developed for potential therapeutic use in the treatment of HDBC and other hormone-dependent malignant diseases.

Experimental Section

General Methods for Synthesis. Unless otherwise stated, HPLC grade solvents were used and commercial reagents and starting materials were used without further purification. Sulfamoyl chloride was prepared by an adaptation of the method of Appel and Berger[47] and was stored at 4 °C under positive N_2 pressure as a solution in toluene, as described by Woo et al.[23] Thin-layer chromatography (TLC) was performed on precoated plates (Merck TLC aluminum sheets silica gel 60 F254, art. no. 5554). Product(s) and starting materials(s) were detected by either viewing under UV light or treatment with an ethanolic solution of phosphomolybdic acid followed by heating. Flash column chromatography was performed on glass columns packed with silica gel (Sorbsil/Matrex C60) or on FlashMaster II run Argonaut prepacked columns or on ISCO CombiFlash Rf automated flash chromatography system run RediSep Rf disposable flash columns. Nuclear magnetic resonance spectra were recorded on either a Jeol Delta 270 MHz or Varian Mercury VX 400 MHz spectrometer. ^{1}H NMR spectra were recorded at 270 or 400 MHz with shifts reported in parts per million (ppm, δ) relative to residual chloroform (δ_H = 7.26 ppm) or residual DMSO (δ_H = 2.50 ppm). Coupling constants, *J*, are reported in hertz. ^{13}C NMR spectra were recorded at either 67.9 or 100.6 MHz with the central peak of chloroform (δ_C = 77.16 ppm) or DMSO (δ_C = 39.52 ppm) as internal standard. The following abbreviations are used to describe resonances in ^{1}H NMR and ^{13}C NMR spectra: br, broad; s, singlet; d, doublet; dd, double doublet; q, quartet; m, multiplet; t, triplet. HPLC analyses were performed on a Waters Millenium 32 instrument equipped with a Waters 996 PDA detector. For chromatographic conditions, refer to Supporting Information. All biologically tested compounds attained a purity level of 95% or above by HPLC. LC-MS analysis was performed on a Waters 2790 Alliance linked up with a ZQ MicroMass spectrometer and a Waters 996 PDA detector. FAB accurate mass spectra were recorded at the EPSRC National Mass Spectrometry Service Centre, University of Wales Swansea, Chemistry Department, using *m*-nitrobenzyl alcohol as the matrix. Atmospheric pressure chemical ionization (APCI) or electrospray (ES) high resolution mass spectra were recorded on a Bruker micrOTOF Focus. Elemental analyses were performed by the Microanalysis Service, University of Bath. Melting points (mp) were determined using a Stanford Research Systems Optimelt MPA100 automated melting point system and are uncorrected. Microwave reactions were carried out using a CEM Discover microwave.

Biology. The extent of in vitro inhibition of STS and aromatase activity by compounds was assessed using JEG-3 human choriocarcinoma cells which were chosen because these cells constitutively express both enzymes maximally. In our hands, these enzyme activities remain stable during repeated subculturing over several months. Cells were seeded into 24-well culture plates and maintained in MEM (Sigma, Poole, UK) containing supplements and used when 80% confluent. To determine STS activity, cells were incubated for 1 h with [6,7-^{3}H]E1S (3 nM, 60 Ci mmol^{-1}; PerkinElmer Life Sciences, Wellesley, MA) in the presence or absence of (0.001−10000 nmol L^{-1}) inhibitor. The product E1 was separated from E1S by toluene partition using [4-^{14}C]E1 to monitor procedural losses, and the radioactivity was measured by scintillation spectrometry. Similarly, for aromatase activity, [1β-^{3}H]androstenedione (2−3 nM, 30 Ci mmol^{-1}; PerkinElmer Life Sciences, Wellesley, MA) was incubated with JEG-3 cells for 1 h in the presence or absence of inhibitor. The product, tritiated water (^3H_2O), was separated using dextran-coated charcoal at 4−8 °C for 2 h, and remaining radioactivity was measured by scintillation spectrometry. Each IC_{50} value represents the mean ± SE of triplicate measurements.

The in vivo inhibition of aromatase and STS activity by letrozole, **9**, **19**, **20**, **22**, and **23** was assessed in immature female Wistar rats (20 days) purchased from Charles River, UK. Animals received a single subcutaneous injection of PMSG, 200 IU, Sigma. Three days later, compounds (1 mg kg^{-1}) and letrozole (0.1 mg kg^{-1}) were administered orally in THF/propylene glycol (10:90) as a single dose. Blood and liver samples were obtained 3 h after drug administration. Plasma concentrations of E2 were measured using a radio-immunoassay kit (Diagnostic Products Corporation, CA) to monitor the extent of aromatase inhibition. Liver STS activity was determined by incubating rat liver homogenate with [^{3}H]E1S [7 × 10^{-5} dpm, 60 Ci mmol^{-1}, adjusted to 20 μM with nonradioactive E1S (Sigma)] for 1 h. The product was extracted with toluene, and the radioactivity was measured by liquid scintillation spectrometry. Results are expressed as the percent inhibition of PMSG-stimulated E2 levels for aromatase activity or the

percent activity in untreated animals for STS activity (mean ± SE, $n = 3-5$).

Uterine Weight Gain Assay. Ovariectomized female Wistar rats (200 g) were purchased from Charles River. Groups of three rats were treated with 10% THF/90% propylene glycol vehicle (po), 1 μg E1/rat (sc in 10% ethanol/90% propylene glycol), or orally with **2** and **23** at 10 mg/kg/d for 4 days. Animals were sacrificed 24 h after administration of the last dose of compound and uteri were removed, excised of fat, and weighed. Total body weights of the rats were also recorded, and the uterine weight was expressed as % total body weight.

hCAII Studies. To assess the inhibition of hCAII in vitro, an adaptation of a colorimetric assay previously developed was used.[48] CAII-catalyzed hydrolysis of *p*-nitrophenyl acetate produces *p*-nitrophenol, which has an absorption peak at 384 nm which allows for colorimetric determination of product and subsequent calculation of enzyme activity.

Inhibition constants (IC_{50} values) were measured based on the method previously described,[28] using a 96-well plate spectrophotometric assay except the initial rates were measured rather than the absorbance after 20 min. Assays contained hCAII (Sigma, 180 nM) and 1 mM 4-nitrophenol acetate in 50 mM Tris-HCl, pH 7.6 in a final volume of 0.20 mL. Initial rates of the enzyme reaction were monitored for 2 min at 20 °C. Stock solutions and dilutions of **23** were prepared in ethanol such that there was a constant 5% ethanol in the assay. At least three replicates at each concentration were used.

Protein Crystallography. The hanging drop vapor diffusion method was used for crystallization. Protein (2.5 μL, ~10 mg/mL, ~0.3 mM) containing 0.5 mM inhibitors and 30 mM 2-mercaptoethanol was mixed with well buffer (2.5 μL; 0.1 M Tris/HCl, pH 8.0, 1 mM $ZnSO_4$, and 2.49 M ammonium sulfate), with crystals appearing after 3−4 weeks at 4 °C.

X-ray diffraction data were collected at station PX14.2 at the Synchrotron Radiation Source (Daresbury, U.K.) under cryogenic conditions with a 5 s exposure and a crystal to detector distance of 168.6 mm, with 100 frames of 1° oscillation collected. Before data collection, the crystals were flash-cooled to 100 K in a cryoprotectant containing the reservoir solution and 33% (v/v) 8 M sodium formate. Data were indexed and reduced with DENZO and SCALEPACK modules of the HKL suite[49] in the orthorhombic $P2_1$ space group. The structure was determined by the molecular replacement method using 1TTM.pdb[41] as the search model with the program Phaser[50] from the CCP4i program suite.[45] Refinement was performed using Refmac5[51] from the program package CCP4i in addition to manual model building using the program COOT.[46] Clear density for the active site zinc, and the inhibitor was observed after the first round of refinement. The topology files for each inhibitor were generated using the Dundee PRODRG2 Server.[52] After alternating cycles of water addition, refinement and manual rebuilding the final inhibitor complex had a final $R_{free} = 0.19$ and $R_{cryst} = 0.15$. The statistics for refinement are summarized in the Supporting Information. Coordinates and structure factors have been deposited with the Protein Data Bank (accession code 2wd3.pdb).

General Method of Sulfamoylation. A solution of sulfamoyl chloride (H_2NSO_2Cl) in toluene (ca. 0.7 M)[23] was concentrated in vacuo at 30 °C to furnish a yellow oil which solidified upon cooling in an ice bath. The substrate in anhydrous *N*,*N*-dimethylacetamide (DMA) was subsequently added, and the reaction mixture was allowed to warm to room temperature and stirred overnight.

3-Hydroxy-4-chlorophenylboronic Acid 17. With stirring and under an atmosphere of N_2, a solution 5-bromo-2-chlorophenol (4.25 g, 20.5 mmol) in anhydrous THF (100 mL) was cooled to −78 °C (dry ice/acetone). After 30 min, *n*-BuLi (16.4 mL, 40.9 mmol, 2.5 M in hexanes) was added dropwise over 30 min. The reaction was left to stir for 1 h. Triisopropyl borate (5.65 mL, 24.6 mmol) was added dropwise with the reaction temperature maintained at −78 °C. After 15 min of stirring at this temperature, the dry ice/acetone bath was removed. At 0 °C, 2 M $HCl_{(aq)}$ was added dropwise until the pH of the reaction mixture was neutral and the reaction left to stir for a further 15 min. THF was removed in vacuo and residues obtained taken up in EtOAc (50 mL). Distilled H_2O (50 mL) was added and the organic layer separated. The aqueous layer was extracted with EtOAc (50 mL × 2) and the organic portions combined, dried ($MgSO_4$), and solvent removed in vacuo. Addition of CH_2Cl_2 (100 mL) to the viscous yellow oil obtained resulted in a white precipitate that was collected via filtration to give **17** as a white solid (0.88 g, 25%), mp >250 °C. ^{1}H NMR δ_H (270 MHz, DMSO-d_6) 7.18−7.32 (m, 3H), 8.06 (s, 2H) and 9.94 (br s, 1H). LCMS ($APCI^-$) *m*/*z* (rel intensity) 173 (25, $[^{37}ClM - H]^-$), 171 (80, $[^{35}ClM - H]^-$), 127 (100 $[(^{35}ClM - H) - B(OH)_2]^-$).

5-((1*H*-1,2,4-Triazol-1-yl)methyl)-4′-hydroxybiphenyl-2-carbonitrile 19. A 10 mL microwave vial was loaded with **10** (0.150 g, 0.570 mmol), 4-hydroxyphenylboronic acid (0.118 g, 0.855 mmol), K_2CO_3 (0.198 g, 1.43 mmol), tetrabutylammonium bromide (0.189 g, 0.570 mmol), distilled H_2O (3.5 mL), and EtOH (1.5 mL). The vial was sealed and loaded (with no prior degassing) into a CEM Discover microwave. After a run time of 5 min at 120 °C (150 W), the reaction mixture was allowed to cool and diluted with EtOAc (50 mL). The resulting mixture was then washed with distilled H_2O (25 mL × 3) and brine (25 mL). The organic layer separated was dried ($MgSO_4$), filtered, and solvent removed in vacuo to leave a yellow/brown residue. Column chromatography (EtOAc) eluted **19** as a white solid (0.102 g, 65%), mp 211−213 °C. ^{1}H NMR δ_H (270 MHz, $CDCl_3$) 5.62 (s, 2H), 6.90 (d, $J = 8.6$, 2H), 7.32 (d, $J = 8.2$, 1H), 7.38 (d, $J = 8.5$, 2H), 7.45 (s, 1H), 7.89 (d, $J = 7.9$, 1H), 8.02 (s, 1H), 8.17 (s, 1H) and 9.87 (br s, 1H). LCMS ($APCI^+$) *m*/*z* (rel intensity) 277 (100, $[M + H]^+$). HRMS (ES^+) *m*/*z* calcd for $C_{16}H_{13}N_4O$ $[M+H]^+$: 277.1084, found 277.1084. Anal. ($C_{16}H_{12}N_4O$) C, H, N.

5′-((1*H*-1,2,4-Triazol-1-yl)methyl)-2′-cyanobiphenyl-4-yl Sulfamate 20. As general method using H_2NSO_2Cl (4.63 mL, 1.39 mmol), DMA (1.5 mL) and **19** (0.077 g, 0.279 mmol). The reaction mixture was poured into EtOAc (30 mL). The organic layer separated was washed with distilled H_2O (30 mL × 4), brine (30 mL), dried ($MgSO_4$), and evaporated in vacuo to give white residues. Column chromatography (CH_2Cl_2/acetone 80:20) eluted **15** as a white solid (0.074 g, 75%), mp 159−162 °C. ^{1}H NMR δ_H (270 MHz, DMSO-d_6) 5.60 (s, 2H), 7.41−7.46 (m, 3H), 7.51 (s, 1H), 7.67 (d, $J = 8.2$, 2H), 7.98 (d, $J = 7.9$, 1H), 8.03 (s, 1H), 8.17 (br s, 2H) and 8.73 (s, 1H). LCMS ($APCI^-$) *m*/*z* (rel intensity) 354 (100, $[M - H]^-$). HRMS (FAB^+) *m*/*z* calcd for $C_{16}H_{14}N_5O_3S$ $(M + H)^+$: 356.0812, found 356.0811.

5′-((1*H*-1,2,4-Triazol-1-yl)methyl)-2′-cyanobiphenyl-4-yl Dimethylsulfamate 21. To a white suspension of **19** (0.075 g, 0.271 mmol) and NEt_3 (0.292 mL, 2.71 mmol) in anhydrous CH_2Cl_2 (2 mL) at 0 °C under an inert atmosphere was added to a colorless solution of *N*,*N*-dimethylsulfamoyl chloride (0.408 mL, 3.80 mmol) in anhydrous CH_2Cl_2 (3 mL). The resulting white suspension was left to stir under an inert atmosphere at room temperature for 70 h, forming a clear orange/brown solution. The reaction mixture was diluted in CH_2Cl_2 (30 mL) and washed with distilled H_2O (30 mL × 3) and brine (30 mL). The organic fraction was separated, dried ($MgSO_4$), filtered, and solvent removed in vacuo to leave yellow residues. Column chromatography (CH_2Cl_2/acetone 75:25) eluted **21** as a viscous yellow oil (0.093 g, 90%). ^{1}H NMR δ_H (270 MHz, $CDCl_3$) 3.00 (s, 6H), 5.44 (s, 2H), 7.28−7.33 (m, 2H), 7.39 (d, $J = 8.7$ Hz, 2H), 7.53 (d, $J = 8.7$ Hz, 2H), 7.76 (d, $J = 7.9$ Hz, 1H), 8.00 (s, 1H) and 8.18 (s, 1H). LCMS ($APCI^-$) *m*/*z* (rel intensity) 382 (100, $[M - H]^-$). HRMS (ES^+) *m*/*z* calcd for $C_{18}H_{18}N_5O_3S$ $[M + H]^+$: 384.1125, found 384.1143.

5-((1*H*-1,2,4-Triazol-1-yl)methyl)-3′-chloro-4′-hydroxybiphenyl-2-carbonitrile 22. The title compound was prepared from **10** and 3-chloro-4-hydroxyphenylboronic acid using similar

conditions to those described for the synthesis of **19**. Chromatography (EtOAc) eluted **22** as a white solid (0.218 g, 62%), mp 188−189 °C. ^{1}H NMR δ_H (270 MHz, DMSO-d_6) 5.56 (s, 2H), 7.10 (d, J = 8.4 Hz, 1H), 7.34−7.39 (m, 2H), 7.52 (d, J = 1.2 Hz, 1H), 7.56 (d, J = 2.2 Hz, 1H), 7.91 (d, J = 7.9 Hz, 1H), 8.02 (s, 1H), 8.72 (s, 1H) and 10.69 (br s, 1H). LCMS (APCI$^-$) m/z (rel intensity) 311 (30, [^{37}ClM − H]$^-$), 309 (100, [^{35}ClM − H]$^-$). HRMS (ES$^+$) m/z calcd for $C_{16}H_{12}ClN_4O$ [M + H]$^+$: 311.0694, found 311.0684. Anal. ($C_{16}H_{11}ClN_4O$) C, H, N.

5′-((1*H*-1,2,4-Triazol-1-yl)methyl)-3-chloro-2′-cyanobiphenyl-4-yl Sulfamate 23. The title compound was prepared from **22** using similar conditions to those described for the synthesis of **20**. Chromatography (CH_2Cl_2/acetone 80:20) eluted **23** as a white solid (0.292 g, 93%), mp 133−136 °C. ^{1}H NMR δ_H (270 MHz, DMSO-d_6) 5.59 (s, 2H), 7.41−7.46 (d, J = 8.2 Hz, 1H), 7.59 (s, 1H), 7.65 (s, 2H), 7.84 (s, 1H), 7.99 (d, J = 7.9 Hz, 1H), 8.03 (s, 1H), 8.45 (br s, 2H) and 8.72 (s, 1H). LCMS (APCI$^+$) m/z (rel intensity) 392 (43, [^{37}ClM + H]$^+$), 390 (100, [^{35}ClM + H]$^+$). HRMS (FAB$^+$) m/z calcd for $C_{16}H_{13}ClN_5O_3S$ [M + H]$^+$: 390.0422, found 390.0421. Anal. ($C_{16}H_{12}ClN_5O_3S$): C, H, N.

5′-((1*H*-1,2,4-Triazol-1-yl)methyl)-3-chloro-2′-cyanobiphenyl-4-yl Dimethylsulfamate 24. The title compound was prepared from **22** using similar conditions to those described for the synthesis of **21**. Chromatography (CH_2Cl_2/acetone 75:25) eluted **24** as a white solid (0.189 g, 60%), mp 119−120 °C. ^{1}H NMR δ_H (270 MHz, $CDCl_3$) 3.07 (s, 6H), 5.45 (s, 2H), 7.30−7.33 (m, 2H), 7.43 (dd, J = 2.2 Hz, 8.4 Hz, 1H), 7.58 (d, J = 2.2 Hz, 1H), 7.62 (d, J = 10.9 Hz, 1H), 7.77 (d, J = 8.7 Hz, 1H), 8.01 (s, 1H) and 8.18 (s, 1H). LCMS (APCI$^-$), m/z 418 (40, [^{37}ClM − H]$^-$), 416 (100, [^{35}ClM$^-$ − H]$^-$). HRMS (ES$^+$) m/z calcd for $C_{18}H_{17}ClN_5O_3S$ [M + H]$^+$: 418.0735, found 418.0725. Anal. ($C_{18}H_{16}ClN_5O_3S$) C, H, N.

5-((1*H*-1,2,4-Triazol-1-yl)methyl)-4′-chloro-3′-hydroxybiphenyl-2-carbonitrile 25. The title compound was prepared from **10** and **17** using similar conditions to those described for the synthesis of **19**. Chromatography (EtOAc) eluted **25** as a white solid (0.111 g, 54%), mp 228−229 °C. ^{1}H NMR δ_H (270 MHz, DMSO-d_6) 5.58 (s, 2H), 6.96 (dd, J = 2.2 Hz, 8.2 Hz, 1H), 7.11 (d, J = 2.2 Hz, 1H), 7.41 (dd, J = 2.2 Hz, 7.9 Hz, 1H), 7.47 (d, J = 8.2 Hz, 1H), 7.50 (d, J = 8.2 Hz, 1H), 7.95 (d, J = 8.2 Hz, 1H), 8.03 (s, 1H), 8.72 (s, 1H) and 10.60 (br s, 1H). LCMS (APCI$^-$) m/z (rel intensity) 311 (25, [^{37}ClM − H]$^-$), 309 (100, [^{35}ClM − H]$^-$). HRMS (ES$^+$) m/z calcd for $C_{16}H_{12}ClN_4O$ [M + H]$^+$: 311.0694, found 311.0680. Anal. ($C_{16}H_{11}ClN_4O$) C, H, N.

5′-((1*H*-1,2,4-Triazol-1-yl)methyl)-4-chloro-2′-cyanobiphenyl-3-yl Sulfamate 26. The title compound was prepared from **25** using similar conditions to those described for the synthesis of **20**. Chromatography (CH_2Cl_2/acetone 80:20) eluted **26** as a white solid (0.087 g, 87%), mp 148−150 °C. ^{1}H NMR δ_H (270 MHz, DMSO-d_6) 5.59 (s, 2H), 7.45 (dd, J = 1.5 Hz, 7.9 Hz, 1H), 7.57 (dd, J = 2.2 Hz, 8.4 Hz, 1H), 7.61 (d, J = 1.5 Hz, 1H), 7.66 (d, J = 2.2 Hz, 1H), 7.80 (d, J = 8.4 Hz, 1H), 8.00 (d, J = 7.9 Hz, 1H), 8.03 (s, 1H), 8.37 (br s, 2H) and 8.72 (s, 1H). LCMS (APCI$^-$) m/z (rel intensity) 390 (20, [^{37}ClM − H]$^-$), 388 (100, [^{35}ClM − H]$^-$). HRMS (ES$^+$) m/z calcd for $C_{16}H_{13}ClN_5O_3S$ [M + H]$^+$: 390.0422, found 390.0421.

3-((1*H*-1,2,4-Triazol-1-yl)methyl)-3′-hydroxybiphenyl-4-carbonitrile 28. The title compound was prepared from **11** and 3-hydroxyphenylboronic acid using similar conditions to those described for the synthesis of **19**. Chromatography (EtOAc) eluted **28** as a white solid (0.184 g, 89%), mp 183−184 °C. ^{1}H NMR δ_H (270 MHz, DMSO-d_6) 5.68 (s, 2H), 6.85 (dd, J = 2.2 Hz, 8.2 Hz, 1H), 7.01−7.10 (m, 2H), 7.30 (t, J = 8.2 Hz, 1H), 7.68 (s, 1H), 7.78 (dd, J = 2.2 Hz, 8.2 Hz, 1H), 7.95 (d, J = 8.2 Hz, 1H), 8.06 (s, 1H), 8.75 (s, 1H) and 9.73 (br s, 1H). LCMS (APCI$^+$) m/z (rel intensity) 277 (100, [M + H]$^+$). HRMS (ES$^+$) m/z calcd for $C_{16}H_{13}N_4O$ [M + H]$^+$: 277.1084, found 277.1071. Anal. ($C_{16}H_{12}N_4O$) C, H, N.

3′-((1*H*-1,2,4-Triazol-1-yl)methyl)-4′-cyanobiphenyl-3-yl Sulfamate 29. The title compound was prepared from **28** using similar conditions to those described for the synthesis of **20**. Chromatography (CH_2Cl_2/acetone 80:20) eluted **29** as a white solid (0.071 g, 92%), mp 137−138 °C. ^{1}H NMR δ_H (270 MHz, DMSO-d_6) 5.69 (s, 2H), 7.38 (d, J = 7.6 Hz, 1H), 7.59−7.69 (m, 3H), 7.83−7.89 (m, 2H), 8.01−8.03 (m, 2H), 8.09 (s, 2H) and 8.74 (s, 1H). LCMS (APCI$^+$) m/z (rel intensity) 356 (100, [M + H]$^+$). HRMS (ES$^+$) m/z calcd for $C_{16}H_{14}N_5O_3S$ [M + H]$^+$: 356.0812, found 356.0811.

3-((1*H*-1,2,4-Triazol-1-yl)methyl)-4′-hydroxybiphenyl-4-carbonitrile 30. The title compound was prepared from **11** and 4-hydroxyphenylboronic acid using similar conditions to those described for the synthesis of **19**. Chromatography (EtOAc) eluted **30** as a white solid (0.082 g, 79%), mp 203−204 °C. ^{1}H NMR δ_H (270 MHz, DMSO-d_6) 5.62 (s, 2H), 6.86 (d, J = 8.7 Hz, 2H), 7.53 (d, J = 8.7 Hz, 2H), 7.67−7.89 (m, 3H), 7.99 (s, 1H), 8.71 (s, 1H) and 9.83 (br s, 1H). LCMS (APCI$^-$) m/z (rel intensity) 275 (100, [M + H]$^+$). HRMS (ES$^+$) m/z calcd for $C_{16}H_{13}N_4O$ [M + H]$^+$: 277.1084, found 277.1080.

3′-((1*H*-1,2,4-Triazol-1-yl)methyl)-4′-cyanobiphenyl-4-yl Sulfamate 31. The title compound was prepared from **30** using similar conditions to those described for the synthesis of **20**. Chromatography (CH_2Cl_2/acetone 80:20) eluted **31** as a white solid (0.106 g, 82%), mp 179−180 °C. ^{1}H NMR δ_H (270 MHz, DMSO-d_6) 5.67 (s, 2H), 7.40 (d, J = 8.7 Hz, 2H), 7.78 (d, J = 8.7 Hz, 2H), 7.82−7.86 (s, 2H), 7.98 (d, J = 8.2 Hz, 1H), 8.01 (s, 1H), 8.08 (s, 2H) and 8.72 (s, 1H). LCMS (APCI$^+$) m/z (rel intensity) 356 (100, [M + H]$^+$). HRMS (ES$^+$) m/z calcd for $C_{16}H_{14}N_5O_3S$ [M + H]$^+$: 356.0812, found 356.0813. Anal. ($C_{16}H_{13}N_5O_3S$) C, H, N.

3-((1*H*-1,2,4-Triazol-1-yl)methyl)-3′-chloro-4′-hydroxybiphenyl-4-carbonitrile 32. The title compound was prepared from **11** and 3-chloro-4-hydroxyphenylboronic acid using similar conditions to those described for the synthesis of **19**. Chromatography (EtOAc) eluted **32** as a white solid (0.065 g, 37%), mp 244−247 °C. ^{1}H NMR δ_H (270 MHz, DMSO-d_6) 5.67 (s, 2H), 7.09 (d, J = 8.4 Hz, 1H), 7.54 (dd, J = 2.2 Hz, 8.2 Hz, 1H), 7.75 (d, J = 2.2 Hz, 1H), 7.80−7.83 (m, 2H), 7.89−7.93 (m, 2H), 8.04 (s, 1H) and 8.73 (br s, 1H). LCMS (APCI$^+$) m/z (rel intensity) 313 (35, [^{37}ClM + H]$^+$), 311 (100, [^{35}ClM + H]$^+$). HRMS (FAB$^+$) m/z calcd for $C_{16}H_{12}ClN_4O$ [M + H]$^+$: 311.0694, found 311.0690. Anal. ($C_{16}H_{11}ClN_4O$) C, H, N.

3′-((1*H*-1,2,4-Triazol-1-yl)methyl)-3-chloro-4′-cyanobiphenyl-4-yl Sulfamate 33. The title compound was prepared from **32** using similar conditions to those described for the synthesis of **20**. Chromatography (CH_2Cl_2/acetone 80:20) eluted **33** as a white solid (0.057 g, 78%), mp 155−158 °C. ^{1}H NMR δ_H (270 MHz, DMSO-d_6) 5.73 (s, 2H), 7.62 (d, J = 8.7 Hz, 1H), 7.78 (d, J = 8.7 Hz, 1H), 7.89−7.98 (m, 4H), 8.01 (s, 1H), 8.38 (br s, 2H) and 8.73 (s, 1H). LCMS (APCI$^+$) m/z (rel intensity) 392 (40, [^{37}ClM + H]$^+$), 390 (100, [^{35}ClM + H]$^+$). HRMS (ES$^+$) m/z calcd for $C_{16}H_{13}ClN_5O_3S$ [M + H]$^+$: 390.0422, found 390.0426.

5-((1*H*-1,2,4-Triazol-1-yl)methyl)biphenyl-3-carbonitrile 34. The title compound was prepared from **12** and phenylboronic acid using similar conditions to those described for the synthesis of **19**. Chromatography ($CHCl_3$/acetone 90:10) eluted **34** as a white solid (0.050 g, 77%), mp 109−110 °C. ^{1}H NMR δ_H (270 MHz, $CDCl_3$) 5.45 (s, 2H), 7.44−7.53 (m, 6H), 7.67 (s, 1H), 7.84 (s, 1H), 8.03 (s, 1H) and 8.19 (s, 1H). LCMS (ES$^-$) m/z (rel intensity) 261 (100, [M + H]$^-$). HRMS (ES$^+$) m/z calcd for $C_{16}H_{13}N_4$ [M + H]$^+$: 261.1135, found 261.1122.

5-((1*H*-1,2,4-Triazol-1-yl)methyl)-4′-fluorobiphenyl-3-carbonitrile 35. The title compound was prepared from **12** and 4-fluorophenylboronic acid using similar conditions to those described for the synthesis of **19**. Chromatography ($CHCl_3$/acetone 90:10) eluted **35** as a white solid (0.040 g, 50%), mp 134−135 °C. ^{1}H NMR δ_H (270 MHz, $CDCl_3$) 5.45 (s, 2H), 7.13−7.21 (m, 2H), 7.46−7.51 (m, 3H), 7.62 (s, 1H), 7.79 (s, 1H), 8.03 (s, 1H) and 8.19 (s, 1H). LCMS (ES$^+$) m/z (rel intensity) 279 (100, [M + H]$^+$). HRMS (ES$^+$) m/z calcd for $C_{16}H_{12}FN_4$ [M + H]$^+$: 279.1041, found 279.1030.

5-((1*H*-1,2,4-Triazol-1-yl)methyl)biphenyl-3,4′-dicarbonitrile 36. The title compound was prepared from **12** and 4-cyanophenylboronic acid using similar conditions to those described for the synthesis of **19**. Chromatography ($CHCl_3$/acetone 80:20) eluted **36** as a white solid (0.038 g, 47%), mp 154−155 °C. ^{1}H NMR δ_H (270 MHz, $CDCl_3$) 5.47 (s, 2H), 7.49−7.67 (m, 4H), 7.76−7.79 (m, 2H), 7.84 (t, J = 1.4 Hz, 1H), 8.03 (s, 1H) and 8.21 (s, 1H). LCMS (ES^+) m/z (rel intensity) 286 (100, $[M + H]^+$). HRMS (ES^+) m/z calcd for $C_{17}H_{12}N_5$ $[M + H]^+$: 286.1087, found 286.1075.

5-((1*H*-1,2,4-Triazol-1-yl)methyl)-4′-hydroxybiphenyl-3-carbonitrile 37. The title compound was prepared from **12** and 4-hydroxyphenylboronic acid using similar conditions to those described for the synthesis of **19**. Chromatography ($CHCl_3$/acetone 80:20) eluted **37** as a white solid (0.086 g, 81%), mp 186−187 °C. ^{1}H NMR δ_H (270 MHz, DMSO-d_6) 5.52 (s, 2H), 6.87 (d, J = 8.5 Hz, 2H), 7.55 (d, J = 8.5 Hz, 2H), 7.62 (s, 1H), 7.86 (s, 1H), 8.02 (s, 2H), 8.72 (s, 1H) and 9.78 (br s, 1H). LCMS (ES^-) m/z (rel intensity) 277 (100, $[M + H]^-$). HRMS (ES^+) m/z calcd for $C_{16}H_{13}N_4O$ $[M + H]^+$: 277.1084, found 277.1071. Anal. ($C_{16}H_{12}N_4O$) C, H, N.

3′-((1*H*-1,2,4-Triazol-1-yl)methyl)-5′-cyanobiphenyl-4-yl Sulfamate 38. The title compound was prepared from **37** using similar conditions to those described for the synthesis of **20**. Chromatography (CH_2Cl_2/MeOH 96:4) eluted **38** as a white solid (0.115 g, 89%), mp 166−167 °C. ^{1}H NMR δ_H (270 MHz, DMSO-d_6) 5.56 (s, 2H), 7.40 (d, J = 8.5 Hz, 2H), 7.76 (s, 1H), 7.81 (d, J = 8.5 Hz, 2H), 7.96 (s, 1H), 8.02 (s, 1H), 8.09 (br s, 2H), 8.15 (s, 1H) and 8.73 (s, 1H). LCMS (ES^+) m/z (rel intensity) 356 (100, $[M + H]^+$). HRMS (ES^+) m/z calcd for $C_{16}H_{14}N_5O_3S$ $[M + H]^+$: 356.0812, found 356.0800.

5-((1*H*-1,2,4-Triazol-1-yl)methyl)-3′-chloro-4′-hydroxybiphenyl-3-carbonitrile 39. The title compound was prepared from **12** and 3-chloro-4-hydroxyphenylboronic acid using similar conditions to those described for the synthesis of **19**. Chromatography ($CHCl_3$/acetone 80:20) eluted **39** as a white solid (0.189 g, 80%), mp 208−209 °C. ^{1}H NMR δ_H (270 MHz, DMSO-d_6) 5.52 (s, 2H), 7.06 (d, J = 8.5 Hz, 1H), 7.53 (dd, J = 2.2 and 8.5 Hz, 1H), 7.65 (s, 1H), 7.76 (d, J = 2.2 Hz, 1H), 7.95 (s, 1H), 8.01 (s, 1H), 8.10 (t, J = 1.6 Hz, 1H) and 8.72 (s, 1H). LCMS (ES^+) m/z (rel intensity) 313 (36, $[^{37}ClM + H]^+$), 311 (100, $[^{35}ClM + H]^+$). HRMS (ES^+) m/z calcd for $C_{16}H_{12}ClN_4O$ $[M + H]^+$: 311.0694, found 311.0686. Anal. ($C_{16}H_{11}ClN_4O$) C, H, N.

3′-((1*H*-1,2,4-Triazol-1-yl)methyl)-3-chloro-5′-cyanobiphenyl-4-yl Sulfamate 40. The title compound was prepared from **39** using similar conditions to those described for the synthesis of **20**. Chromatography ($CHCl_3$/acetone 80:20) eluted **40** as a white solid (0.120 g, 87%), mp 163−164 °C. ^{1}H NMR δ_H (270 MHz, DMSO-d_6) 5.55 (s, 2H), 7.61 (d, J = 8.8 Hz, 1H), 7.77−7.80 (m, 2H), 8.00−8.04 (m, 3H), 8.22 (s, 1H), 8.36 (br s, 2H) and 8.72 (s, 1H). LCMS (ES^+) m/z (rel intensity) 392 (38, $[^{37}ClM + H]^+$), 390 (100, $[^{35}ClM + H]^+$), 313 (18, $[^{37}ClM - SO_2NH_2]^+$), 311 (56, $[^{35}ClM - SO_2NH_2]^+$). HRMS (ES^+) m/z calcd for $C_{16}H_{13}ClN_5O_3S$ $[M + H]^+$: 390.0422, found 390.0408. Anal. ($C_{16}H_{12}ClN_5O_3S$) C, H. N.

3′-((1*H*-1,2,4-Triazol-1-yl)methyl)biphenyl-4-ol 42. Compound **13** (0.100 g 4.20 mmol), 4-hydroxyphenylboronic acid (0.087 g, 0.630 mmol), K_2CO_3 (0.145 g, 1.05 mmol), tetrabutylammonium bromide (0.139 g, 0.420 mmol), distilled H_2O (7 mL), and EtOH (3 mL) were combined and degassed with N_2 for 30 min. $Pd(OAc)_2$ (3 mol %) was added and the reaction mixture heated with vigorous stirring at 70 °C for 1 h. Upon cooling, EtOAc (50 mL) was added and washed with distilled H_2O (50 mL × 2) and brine (50 mL). The organic portion was separated and dried ($MgSO_4$), filtered, and solvent removed in vacuo to leave a yellow/brown residue. Column chromatography (EtOAc) eluted **42** as a white solid (0.092 g, 88%), mp 163−164 °C. ^{1}H NMR δ_H (270 MHz, DMSO-d_6) 5.44 (s, 2H), 6.83 (d, J = 8.7 Hz, 2H), 7.15 (d, J = 7.7 Hz, 1H), 7.34−7.51 (m, 5H), 7.92 (s, 1H), 8.68 (s, 1H) and 9.58 (br s, 1H). LCMS ($APCI^+$) m/z (rel. intensity) 251 (18, $[M]^+$). HRMS (ES^+) m/z calcd for $C_{15}H_{14}N_3O$ $[M + H]^+$: 252.1131, found 252.1144. Anal. ($C_{15}H_{13}N_3O$) C, H, N.

3′-((1*H*-1,2,4-Triazol-1-yl)methyl)biphenyl-4-yl Sulfamate 43. The title compound was prepared from **42** using similar conditions to those described for the synthesis of **20**. Column chromatography (CH_2Cl_2/acetone 80:20) eluted **43** (0.055 g, 71%) as a white solid, mp 149−152 °C. ^{1}H NMR δ_H (400 MHz, DMSO-d_6) 5.51 (s, 2H), 7.29 (d, J = 7.5 Hz, 1H), 7.39 (d, J = 8.7 Hz, 2H), 7.48 (t, J = 7.5 Hz, 1H), 7.60−7.64 (m, 2H), 7.73 (d, J = 8.7 Hz, 2H), 8.01 (s, 1H), 8.07 (br s, 2H) and 8.73 (s, 1H). LCMS (ES^-) m/z (rel intensity) 329 (100, $[M - H]^-$). HRMS (FAB^+) m/z calcd for $C_{15}H_{14}N_4O_3S$ $[M]^+$: 330.0787, found 330.0782.

3′-((1*H*-1,2,4-Triazol-1-yl)methyl)-3-chlorobiphenyl-4-ol 44. The title compound was prepared from **13** and 3-chloro-4-hydroxyphenylboronic acid using similar conditions to those described for the synthesis of **19**. Column chromatography (EtOAc) eluted **44** as a white solid (0.129 g, 72%), mp 153−154 °C. ^{1}H NMR δ_H (270 MHz, DMSO-d_6) 5.54 (s, 2H), 7.05 (d, J = 8.4 Hz, 1H), 7.19 (d, J = 7.4 Hz, 1H), 7.36−7.45 (m, 2H), 7.55 (d, J = 7.4 Hz, 2H), 7.61 (d, J = 2.2 Hz, 1H), 7.99 (s, 1H), 8.70 (s, 1H) and 10.36 (br s, 1H). LCMS ($APCI^-$) m/z (rel intensity) 286 (30, $[^{37}ClM - H]^-$), 284 (100, $[^{35}ClM - H]^-$). HRMS (ES^+) m/z calcd for $C_{15}H_{13}ClN_3O$ $[M + H]^+$: 286.0742, found 286.0737.

3′-((1*H*-1,2,4-Triazol-1-yl)methyl)-3-chlorobiphenyl-4-yl Sulfamate 45. The title compound was prepared from **44** using similar conditions to those described for the synthesis of **20**. Chromatography (CH_2Cl_2/acetone 80:20) eluted **45** as a white solid (0.055 g, 62%), mp 144−147 °C. ^{1}H NMR δ_H (270 MHz, DMSO-d_6) 5.49 (s, 2H), 7.29 (d, J = 7.4 Hz, 1H), 7.47 (t, J = 5.9 Hz, 1H), 7.57−7.72 (m, 4H), 7.87 (d, J = 2.0 Hz, 1H), 8.00 (s, 1H), 8.34 (br s, 2H) and 8.72 (s, 1H). LCMS ($APCI^+$) m/z (rel intensity) 367 (20, $[^{37}ClM + H]^+$), 365 (55, $[M + H]^+$), 288 (30, $[^{37}ClM - SO_2NH_2]^+$), 286 (100, $[^{35}ClM - SO_2NH_2]^+$). HRMS (ES^+) m/z calcd for $C_{15}H_{14}ClN_4O_3S$ $[M + H]^+$: 365.0470, found 365.0471.

4-((1*H*-1,2,4-Triazol-1-yl)methyl)-4′-hydroxybiphenyl-2-carbonitrile 47. The title compound was prepared from **14** and 4-hydroxyphenylboronic acid using similar conditions to those described for the synthesis of **19**. Chromatography (EtOAc)) eluted **47** as a white solid (0.061 g, 60%), mp 168−171 °C. ^{1}H NMR δ_H (270 MHz, DMSO-d_6) 5.51 (s, 2H), 6.89 (d, J = 8.7 Hz, 2H), 7.40 (d, J = 8.7 Hz, 2H), 7.56 (d, J = 8.2 Hz, 1H), 7.62 (dd, J = 2.0 Hz, 8.2 Hz, 1H), 7.84 (d, J = 2.0 Hz, 1H), 8.02 (s, 1H), 8.72 (s, 1H) and 9.85 (br s, 1H). LCMS ($APCI^-$) m/z (rel intensity) 275 (100, $[M - H]^-$). HRMS (FAB^+) calcd for $C_{16}H_{13}N_4O$ $[M + H]^+$: 277.1084, found 277.1077. Anal. ($C_{16}H_{12}N_4O$) C, H, N.

4′-((1*H*-1,2,4-Triazol-1-yl)methyl)-2′-cyanobiphenyl-4-yl Sulfamate 48. The title compound was prepared from **47** using similar conditions to those described for the synthesis of **20**. Chromatography (CH_2Cl_2/acetone 80:20) eluted **48** a white solid (0.051 g, 66%), mp 157−160 °C. ^{1}H NMR δ_H (270 MHz, DMSO-d_6) 5.55 (s, 2H), 7.43 (d, J = 8.6 Hz, 2H), 7.62−7.70 (m, 4H), 7.92 (s, 1H), 8.03 (s, 1H), 8.16 (br s, 2H) and 8.73 (s, 1H); LCMS ($APCI^-$) m/z (rel intensity) 354 (100, $[M - H]^-$). HRMS (FAB^+) calcd for $C_{16}H_{14}N_5O_3S$ $[M + H]^+$: 356.0812, found 356.0759.

4-((1*H*-1,2,4-Triazol-1-yl)methyl)-3′-chloro-4′-hydroxybiphenyl-2-carbonitrile 49. The title compound was prepared from **14** and 3-chloro-4-hydroxyphenylboronic acid using similar conditions to those described for the synthesis of **19**. Chromatography (EtOAc) eluted **49** as a white solid (0.072 g, 41%), mp 195−197 °C. ^{1}H NMR δ_H (270 MHz, DMSO-d_6) 5.51 (s, 2H), 7.09 (d, J = 8.4 Hz, 1H), 7.37 (dd, J = 2.2 Hz, 8.7 Hz, 1H), 7.57−7.61 (m, 3H), 7.86 (s, 1H), 8.02 (s, 1H), 8.72 (s, 1H) and 10.68 (br s, 1H). LCMS ($APCI^-$) m/z (rel intensity) 311 (25, $[^{37}ClM - H]^-$), 309 (100, $[^{35}ClM - H]^-$). HRMS (ES^+) m/z calcd for $C_{16}H_{12}ClN_4O$ $[M + H]^+$: 311.0694, found 311.0681.

4′-((1*H*-1,2,4-Triazol-1-yl)methyl)-3-chloro-2′-cyanobiphenyl-4-yl Sulfamate 50. The title compound was prepared from **49** using similar conditions to those described for the synthesis of **20**. Chromatography (CH_2Cl_2/acetone 80:20) eluted **50** as a white solid (0.071 g, 82%), mp 151−153 °C. ^{1}H NMR δ_H (270 MHz, DMSO-d_6) 5.55 (s, 2H), 7.61−7.68 (m, 4H), 7.87 (t, J = 1.0 Hz, 1H), 7.94 (s, 1H), 8.04 (s, 1H), 8.43 (br s, 2H) and 8.74 (s, 1H). LCMS (APCI$^-$) m/z (rel intensity) 391 (20, [^{37}ClM − H]$^-$), 388 (100, [^{35}ClM − H]$^-$). HRMS (ES$^+$) m/z calcd for $C_{16}H_{13}ClN_5O_3S$ [M + H]$^+$: 390.0422, found 390.0418.

6-((1*H*-1,2,4-Triazol-1-yl)methyl)-3′-chloro-4′-hydroxybiphenyl-3-carbonitrile 52. The title compound was prepared from **15** and 3-chloro-4-hydroxyphenylboronic acid using similar conditions to those described for the synthesis of **19**. Chromatography (EtOAc) eluted **52** as a white crystalline solid (0.089 g, 46%), mp 243−245 °C. ^{1}H NMR δ_H (270 MHz, DMSO-d_6) 5.46 (s, 2H), 7.05 (d, J = 8.4 Hz, 1H), 7.15−7.23 (m, 2H), 7.44 (d, J = 2.2 Hz, 1H), 7.75 (d, J = 1.7 Hz, 1H), 7.80 (dd, J = 1.7 Hz, 7.9 Hz, 1H), 7.98 (s, 1H), 8.43 (s, 1H) and 10.51 (br s, 1H). LCMS (APCI$^-$) m/z (rel intensity) 311 (35, [^{37}ClM − H]$^-$), 309 (100, [^{35}ClM − H]$^-$). HRMS (ES$^+$) m/z calcd for $C_{16}H_{12}ClN_4O$ [M + H]$^+$: 311.0694, found 311.0689.

2′-((1*H*-1,2,4-Triazol-1-yl)methyl)-3-chloro-5′-cyanobiphenyl-4-yl Sulfamate 53. The title compound was prepared from **52** using similar conditions to those described for the synthesis of **20**. Chromatography (CH_2Cl_2/acetone 80:20) eluted **53** as a white solid (0.051 g, 82%), mp 139−142 °C. ^{1}H NMR δ_H (270 MHz, DMSO-d_6) 5.47 (s, 2H), 7.26 (d, J = 7.9 Hz, 1H), 7.52 (dd, J = 2.2 Hz, 8.4 Hz, 1H), 7.60 (d, J = 8.4 Hz, 1H), 7.73 (d, J = 2.2 Hz, 1H), 7.83 (d, J = 1.7 Hz, 1H), 7.90 (dd, J = 1.7 Hz, 7.9 Hz, 1H), 7.99 (s, 1H), 8.38 (br s, 2H) and 8.45 (s, 1H). LCMS (APCI$^-$) m/z (rel intensity) 390 (20, [^{37}ClM − H]$^-$), 388 (60, [^{35}ClM − H]$^-$), 311 (35 [^{37}ClM − SO_2NH_2]$^-$), 309 (100, [^{35}ClM − SO_2NH_2]$^-$). HRMS (ES$^+$) m/z calcd for $C_{16}H_{13}ClN_5O_3S$ [M + H]$^+$: 390.0422, found 390.0405.

2-(5-((1*H*-1,2,4-Triazol-1-yl)methyl)-4′-hydroxybiphenyl-3-yl)-2-methylpropanenitrile 55. The title compound was prepared from **16** and 4-hydroxyphenylboronic acid using similar conditions to those described for the synthesis of **19**. Chromatography (EtOAc) eluted **55** as a pale-yellow solid (0.216 g, 89%), mp 66−68 °C. ^{1}H NMR δ_H (270 MHz, DMSO-d_6) 1.71 (s, 6H), 5.49 (s, 2H), 6.86 (d, J = 8.7 Hz, 2H), 7.38 (s, 1H), 7.42 (s, 1H), 7.46 (d, J = 8.7 Hz, 2H), 7.59 (s, 1H), 8.00 (s, 1H), 8.72 (s, 1H) and 9.64 (br s, 1H). LCMS (APCI$^-$) m/z (rel intensity) 317 (100, [M − H]$^-$). HRMS (ES$^+$) m/z calcd for $C_{19}H_{19}N_4O$ [M + H]$^+$: 319.1553, found 319.1550.

3′-((1*H*-1,2,4-Triazol-1-yl)methyl)-5′-(2-cyanopropan-2-yl)biphenyl-4-yl Sulfamate 56. The title compound was prepared from **55** using similar conditions to those described for the synthesis of **20**. Chromatography (CH_2Cl_2/acetone 75:25) eluted **56** as a white solid (0.111 g, 86%), mp 74−76 °C. ^{1}H NMR δ_H (270 MHz, DMSO-d_6) 1.72 (s, 6H), 5.52 (s, 2H), 7.37 (d, J = 8.7 Hz, 2H), 7.49 (s, 1H), 7.67 (s, 1H), 7.71 (d, J = 8.7 Hz, 2H), 7.99 (s, 1H), 8.04 (br s, 2H) and 8.71 (s, 1H). LCMS (APCI$^+$) m/z (rel intensity) 398 (100, [M + H]$^+$). HRMS (ES$^+$) m/z calcd for $C_{19}H_{20}N_5O_3S$ [M + H]$^+$: 398.1281, found 398.1273.

2-(5-((1*H*-1,2,4-Triazol-1-yl)methyl)-3′-chloro-4′-hydroxybiphenyl-3-yl)-2-methylpropane-nitrile 57. The title compound was prepared from **16** and 3-chloro-4-hydroxyphenylboronic acid using similar conditions to those described for the synthesis of **19**. Chromatography (EtOAc) eluted **57** as a white solid (0.175 g, 75%), mp 136−138 °C. ^{1}H NMR δ_H (270 MHz, DMSO-d_6) 1.72 (s, 6H), 5.49 (s, 2H), 7.07 (d, J = 8.4 Hz, 1H), 7.42−7.51 (m, 3H), 7.64−7.68 (m, 2H), 8.02 (s, 1H), 8.73 (s, 1H) and 10.44 (br s, 1H). LCMS (APCI$^-$) m/z (rel intensity) 353 (35, [^{37}ClM − H]$^-$), 351 (100, [^{35}ClM − H]$^-$). HRMS (ES$^+$) m/z calcd for $C_{19}H_{18}ClN_4O$ [M + H]$^+$: 353.1164, found 353.1160.

3′-((1*H*-1,2,4-Triazol-1-yl)methyl)-3-chloro-5′-(2-cyanopropan-2-yl)biphenyl-4-yl Sulfamate 58. The title compound was prepared from **57** using similar conditions to those described for the synthesis of **20**. Chromatography (CH_2Cl_2/acetone 80:20) eluted **58** as a white solid (0.097 g, 88%), mp 71−74 °C. ^{1}H NMR δ_H (270 MHz, DMSO-d_6) 1.74 (s, 6H), 5.53 (s, 2H), 7.53 (s, 1H), 7.58−7.61 (m, 2H), 7.71 (d, J = 2.2 Hz, 1H), 7.73 (s, 1H), 7.94 (d, J = 2.2 Hz, 1H), 8.01 (s, 1H), 8.35 (s, 2H) and 8.74 (s, 1H). LCMS (APCI$^-$) m/z (rel intensity) 432 (15, [^{37}ClM − H]$^-$), 430 (35, [^{35}ClM − H]$^-$), 353 (32, [^{37}ClM − SO_2NH_2]$^-$), 351 (100, [^{35}ClM − SO_2NH_2]$^-$). HRMS (ES$^+$) m/z calcd for $C_{19}H_{19}ClN_5O_3S$ [M + H]$^+$: 432.0892, found 432.0889.

Acknowledgment. This work was supported by Sterix Ltd., which is part of the Ipsen group. We thank A. C. Smith for technical support and C. M. Parker for assistance in preparing the manuscript.

Supporting Information Available: ^{13}C NMR data for **19**−**26**, **28**−**40**, **42**, **43**, **45**, **48**−**50**, **52**, **53**, and **55**−**58**. Combustion analysis of **19**, **22**−**25**, **28**, **31**, **32**, **37**, **39**, **40**, **42**, and **47**. HPLC and purity data of biologically tested compounds without combustion analysis. Crystallographic statistics of data collection and refinement for the hCA II−**23** complex. This material is available free of charge via the Internet at http://pubs.acs.org.

References

(1) Recanatini, M.; Cavalli, A.; Valenti, P. Nonsteroidal aromatase inhibitors: recent advances. *Med. Res. Rev.* **2002**, *22*, 282–304.
(2) Brueggemeier, R. W.; Hackett, J. C.; Diaz-Cruz, E. S. Aromatase inhibitors in the treatment of breast cancer. *Endocr. Rev.* **2005**, *26*, 331–345.
(3) Woo, L. W. L. Enzyme Inhibitors Examples for the Treatment of Breast Cancer. In *Enzymes and Their Inhibition: Drug Development*; Smith, H. J. Simons, C., Eds.; CRC Press LLC: Boca Raton, FL, 2005; pp 221−241.
(4) Reed, M. J.; Purohit, A.; Woo, L. W. L.; Newman, S. P.; Potter, B. V. L. Steroid sulfatase: molecular biology, regulation, and inhibition. *Endocr. Rev.* **2005**, *26*, 171–202.
(5) Woo, L. W. L.; Purohit, A.; Malini, B.; Reed, M. J.; Potter, B. V. L. Potent active site-directed inhibition of steroid sulphatase by tricyclic coumarin-based sulphamates. *Chem. Biol.* **2000**, *7*, 773–791.
(6) Stanway, S. J.; Purohit, A.; Woo, L. W. L.; Sufi, S.; Vigushin, D.; Ward, R.; Wilson, R. H.; Stanczyk, F. Z.; Dobbs, N.; Kulinskaya, E.; Elliott, M.; Potter, B. V. L.; Reed, M. J.; Coombes, R. C. Phase I study of STX 64 (667 Coumate) in breast cancer patients: the first study of a steroid sulfatase inhibitor. *Clin. Cancer Res.* **2006**, *12*, 1585–1592.
(7) Stanway, S. J.; Delavault, P.; Purohit, A.; Woo, L. W. L.; Thurieau, C.; Potter, B. V. L.; Reed, M. J. Steroid sulfatase: a new target for the endocrine therapy of breast cancer. *Oncologist* **2007**, *12*, 370–374.
(8) (a) Morphy, R.; Rankovic, Z. Designed multiple ligands. an emerging drug discovery paradigm. *J. Med. Chem.* **2005**, *48*, 6523–6543. (b) Espinoza-Fonseca, L. M. The benefits of the multi-target approach in drug design and discovery. *Bioorg. Med. Chem.* **2006**, *14*, 896–897. (c) Baraldi, P. G.; Preti, D.; Fruttarolo, F.; Tabrizi, M. A.; Romagnoli, R. Hybrid molecules between distamycin A and active moieties of antitumor agents. *Bioorg. Med. Chem.* **2007**, *15*, 17–35. (d) Chen, L.; Wilson, D.; Jayaram, H. N.; Pankiewicz, K. W. Dual inhibitors of inosine monophosphate dehydrogenase and histone deacetylases for cancer treatment. *J. Med. Chem.* **2007**, *50*, 6685–6691. (e) Apsel, B.; Blair, J. A.; Gonzalez, B.; Nazif, T. M.; Feldman, M. E.; Aizenstein, B.; Hoffman, R.; Williams, R. L.; Shokat, K. M.; Knight, Z. A. Targeted polypharmacology: discovery of dual inhibitors of tyrosine and phosphoinositide kinases. *Nat. Chem. Biol.* **2008**, *4*, 691–699. (f) Meunier, B. Hybrid molecules with a dual mode of action: dream or reality? *Acc. Chem. Res.* **2008**, *41*, 69–77. (g) Marques, S. M.; Nuti, E.; Rossello, A.; Supuran, C. T.; Tuccinardi, T.; Martinelli, A.; Santos, M. A. Dual inhibitors of matrix metalloproteinases and carbonic anhydrases: iminodiacetyl-based hydroxamate-benzenesulfonamide conjugates. *J. Med. Chem.* **2008**, *51*, 7968–7979. (h) Wei, D.; Jiang, X.; Zhou, L.; Chen, J.; Chen, Z.; He, C.; Yang, K.; Liu, Y.; Pei, J.; Lai, L. Discovery of multitarget inhibitors by combining molecular docking with common pharmacophore matching. *J. Med. Chem.* **2008**, *51*, 7882–7888. (i) Gangjee, A.; Li, W.; Yang, J.; Kisliuk, R. L. Design, synthesis, and biological

evaluation of classical and nonclassical 2-amino-4-oxo-5-substituted-6-methylpyrrolo[3,2-*d*]pyrimidines as dual thymidylate synthase and dihydrofolate reductase inhibitors. *J. Med. Chem.* **2008**, *51*, 68–76. (j) Gemma, S.; Campiani, G.; Butini, S.; Joshi, B. P.; Kukreja, G.; Coccone, S. S.; Persico, M. B. M.; Nacci, V.; Novellino, I. F. E.; Taramelli, D.; Basilico, N.; Parapini, S.; Yardley, V.; Croft, S.; Keller-Maerki, S.; Rottmann, M.; Brun, R.; Coletta, M.; Marini, S.; Guiso, G.; Caccia, S.; Fattorusso, C. Combining 4-aminoquinoline- and clotrimazole-based pharmacophores toward innovative and potent hybrid antimalarials. *J. Med. Chem.* **2009**, *52*, 502–513. (k) Gediya, L. K.; Njar, V. C. O. Promise and challenges in drug discovery and development of hybrid anticancer drugs. *Expert Opin. Drug Discovery* **2009**, *4*, 1099–1111.

(9) Woo, L. W. L.; Sutcliffe, O. B.; Bubert, C.; Grasso, A.; Chander, S. K.; Purohit, A.; Reed, M. J.; Potter, B. V. L. First dual aromatase-steroid sulfatase inhibitors. *J. Med. Chem.* **2003**, *46*, 3193–3196.

(10) Woo, L. W. L.; Bubert, C.; Sutcliffe, O. B.; Smith, A.; Chander, S. K.; Mahon, M. F.; Purohit, A.; Reed, M. J.; Potter, B. V. L. Dual aromatase-steroid sulfatase inhibitors. *J. Med. Chem.* **2007**, *50*, 3540–3560.

(11) Bubert, C.; Woo, L. W. L.; Sutcliffe, O. B.; Mahon, M. F.; Chander, S. K.; Purohit, A.; Reed, M. J.; Potter, B. V. L. Synthesis of aromatase inhibitors and dual aromatase steroid sulfatase inhibitors by linking an arylsulfamate motif to 4-(4*H*-1,2,4-triazol-4-ylamino)benzonitrile: SAR, crystal structures, in vitro and in vivo activities. *ChemMedChem* **2008**, *3*, 1708–1730.

(12) Wood, P. M.; Woo, L. W. L.; Humphreys, A.; Chander, S. K.; Purohit, A.; Reed, M. J.; Potter, B. V. L. A letrozole-based dual aromatase-sulphatase inhibitor with in vivo activity. *J. Steroid Biochem. Mol. Biol.* **2005**, *94*, 123–130.

(13) Wood, P. M.; Woo, L. W. L.; Labrosse, J. R.; Trusselle, M. N.; Abbate, S.; Longhi, G.; Castiglioni, E.; Lebon, F.; Purohit, A.; Reed, M. J.; Potter, B. V. L. Chiral aromatase and dual aromatase-steroid sulfatase inhibitors from the letrozole template: synthesis, absolute configuration, and in vitro activity. *J. Med. Chem.* **2008**, *51*, 4226–4238.

(14) Jackson, T.; Woo, L. W. L.; Trusselle, M. N.; Chander, S. K.; Purohit, A.; Reed, M. J.; Potter, B. V. L. Dual aromatase-sulfatase inhibitors based on the anastrozole template: synthesis, in vitro SAR, molecular modelling and in vivo activity. *Org. Biomol. Chem.* **2007**, *5*, 2940–2952.

(15) Okada, M.; Nakagawa, T.; Iwashita, S.; Takegawa, S.; Fujii, T.; Koizumi, N. Development of novel steroid sulfatase inhibitors. I. Synthesis and biological evaluation of biphenyl-4-*O*-sulfamates. *J. Steroid Biochem. Mol. Biol.* **2003**, *87*, 141–148.

(16) Jackson, T.; Woo, L. W. L.; Trusselle, M. N.; Purohit, A.; Reed, M. J.; Potter, B. V. L. Non-steroidal aromatase inhibitors based on a biphenyl scaffold: synthesis, in vitro SAR, and molecular modelling. *ChemMedChem* **2008**, *3*, 603–618.

(17) Miyaura, N.; Suzuki, A. Palladium-Catalyzed Cross-Coupling Reactions of Organoboron Compounds. *Chem. Rev.* **1995**, *95*, 2457–2483.

(18) Kotha, S.; Lahiri, K.; Kashinath, D. Recent applications of the Suzuki−Miyaura cross-coupling reaction in organic synthesis. *Tetrahedron* **2002**, *58*, 9633–9695.

(19) Bellina, F.; Carpita, A.; Rossi, R. Palladium Catalysts for the Suzuki Cross-Coupling Reaction: An Overview of Recent Advances. *Synthesis* **2004**, 2419–2440.

(20) Fisher, T. H.; Dershem, S. M.; Prewitt, M. L. Meta-substituent effects on benzyl free-radical stability. *J. Org. Chem.* **1990**, *55*, 1040–1043.

(21) Kappe, C. O.; Dallinger, D. The impact of microwave synthesis on drug discovery. *Nat. Rev. Drug Discovery* **2006**, *5*, 51–63.

(22) Okada, M.; Iwashita, S.; Koizumi, N. Efficient general method for sulfamoylation of a hydroxyl group. *Tetrahedron Lett.* **2000**, *41*, 7047–7051.

(23) Woo, L. W. L.; Lightowler, M.; Purohit, A.; Reed, M. J.; Potter, B. V. L. Heteroatom-substituted analogues of the active-site directed inhibitor estra-1,3,5(10)-trien-17-one-3-sulphamate inhibit estrone sulphatase by a different mechanism. *J. Steroid Biochem. Mol. Biol.* **1996**, *57*, 79–88.

(24) Woo, L. W. L.; Howarth, N. M.; Purohit, A.; Hejaz, H. A.; Reed, M. J.; Potter, B. V. L. Steroidal and nonsteroidal sulfamates as potent inhibitors of steroid sulfatase. *J. Med. Chem.* **1998**, *41*, 1068–1083.

(25) Reed, J. E.; Woo, L. W. L.; Robinson, J. J.; Leblond, B.; Leese, M. P.; Purohit, A.; Reed, M. J.; Potter, B. V. L. 2-Difluoromethyloestrone 3-*O*-sulphamate, a highly potent steroid sulphatase inhibitor. *Biochem. Biophys. Res. Commun.* **2004**, *317*, 169–175.

(26) Bojarova, P.; Denehy, E.; Walker, I.; Loft, K.; De Souza, D. P.; Woo, L. W. L.; Potter, B. V. L.; McConville, M. J.; Williams, S. J. Direct evidence for ArO−S bond cleavage upon inactivation of *Pseudomonas aeruginosa* arylsulfatase by aryl sulfamates. *ChemBioChem* **2008**, *9*, 613–623.

(27) Woo, L. W. L.; Purohit, A.; Reed, M. J.; Potter, B. V. L. Oestrone 3-*O*-(*N*-acetyl)sulphamate, a potential molecular probe of the active site of oestrone sulphatase. *Bioorg. Med. Chem. Lett.* **1997**, *7*, 3075–3080.

(28) Ho, Y. T.; Purohit, A.; Vicker, N.; Newman, S. P.; Robinson, J. J.; Leese, M. P.; Ganeshapillai, D.; Woo, L. W. L.; Potter, B. V. L.; Reed, M. J. Inhibition of carbonic anhydrase II by steroidal and non-steroidal sulphamates. *Biochem. Biophys. Res. Commun.* **2003**, *305*, 909–914.

(29) Purohit, A.; Chander, S. K.; Woo, L. W. L.; Parsons, M. F.; Jhalli, R.; Potter, B. V. L.; Reed, M. J. Inhibition of steroid sulphatase activity via the percutaneous route: a new option for breast cancer therapy. *Anticancer Res.* **2008**, *28*, 1517–1523.

(30) Chander, S. K.; Purohit, A.; Woo, L. W. L.; Potter, B. V. L.; Reed, M. J. The role of steroid sulphatase in regulating the oestrogenicity of oestrogen sulphamates. *Biochem. Biophys. Res. Commun.* **2004**, *322*, 217–222.

(31) Fischer, D. S.; Chander, S. K.; Woo, L. W. L.; Fenton, J. C.; Purohit, A.; Reed, M. J.; Potter, B. V. L. Novel D-ring modified steroid derivatives as potent, non-estrogenic, steroid sulfatase inhibitors with in vivo activity. *J. Steroid Biochem. Mol. Biol.* **2003**, *84*, 343–349.

(32) Fischer, D. S.; Woo, L. W. L.; Mahon, M. F.; Purohit, A.; Reed, M. J.; Potter, B. V. L. D-Ring modified estrone derivatives as novel potent inhibitors of steroid sulfatase. *Bioorg. Med. Chem.* **2003**, *11*, 1685–1700.

(33) Woo, L. W. L.; Fischer, D. S.; Sharland, C. M.; Trusselle, M.; Foster, P. A.; Chander, S. K.; Di Fiore, A.; Supuran, C. T.; De Simone, G.; Purohit, A.; Reed, M. J.; Potter, B. V. L. Anticancer steroid sulfatase inhibitors: synthesis of a potent fluorinated second-generation agent, in vitro and in vivo activities, molecular modeling, and protein crystallography. *Mol. Cancer Ther.* **2008**, *7*, 2435–2444.

(34) Lesuisse, D.; Gourvest, J. F.; Albert, E.; Doucet, B.; Hartmann, C.; Lefrancois, J. M.; Tessier, S.; Tric, B.; Teutsch, G. Biphenyls as surrogates of the steroidal backbone. Part 2: discovery of a novel family of non-steroidal 5α-reductase inhibitors. *Bioorg. Med. Chem. Lett.* **2001**, *11*, 1713–1716.

(35) Edsall, R. J., Jr.; Harris, H. A.; Manas, E. S.; Mewshaw, R. E. ERβ ligands. Part 1: the discovery of ERβ selective ligands which embrace the 4-hydroxybiphenyl template. *Bioorg. Med. Chem.* **2003**, *11*, 3457–3474.

(36) Vicker, N.; Ho, Y.; Robinson, J.; Woo, L. W. L.; Purohit, A.; Reed, M. J.; Potter, B. V. L. Docking studies of sulphamate inhibitors of estrone sulphatase in human carbonic anhydrase II. *Bioorg. Med. Chem. Lett.* **2003**, *13*, 863–865.

(37) Abbate, F.; Winum, J. Y.; Potter, B. V. L.; Casini, A.; Montero, J. L.; Scozzafava, A.; Supuran, C. T. Carbonic anhydrase inhibitors: X-ray crystallographic structure of the adduct of human isozyme II with EMATE, a dual inhibitor of carbonic anhydrases and steroid sulfatase. *Bioorg. Med. Chem. Lett.* **2004**, *14*, 231–234.

(38) Leese, M. P.; Leblond, B.; Smith, A.; Newman, S. P.; Di Fiore, A.; De Simone, G.; Supuran, C. T.; Purohit, A.; Reed, M. J.; Potter, B. V. L. 2-Substituted estradiol bis-sulfamates, multitargeted antitumor agents: synthesis, in vitro SAR, protein crystallography, and in vivo activity. *J. Med. Chem.* **2006**, *49*, 7683–7696.

(39) Leese, M. P.; Jourdan, F. L.; Gaukroger, K.; Mahon, M. F.; Newman, S. P.; Foster, P. A.; Stengel, C.; Regis-Lydi, S.; Ferrandis, E.; Di Fiore, A.; De Simone, G.; Supuran, C. T.; Purohit, A.; Reed, M. J.; Potter, B. V. L. Structure−activity relationships of C-17 cyano-substituted estratrienes as anticancer agents. *J. Med. Chem.* **2008**, *51*, 1295–1308.

(40) Ireson, C. R.; Chander, S. K.; Purohit, A.; Parish, D. C.; Woo, L. W. L.; Potter, B. V. L.; Reed, M. J. Pharmacokinetics of the nonsteroidal steroid sulphatase inhibitor 667 COUMATE and its sequestration into red blood cells in rats. *Br. J. Cancer* **2004**, *91*, 1399–1404.

(41) Lloyd, M. D.; Pederick, R. L.; Natesh, R.; Woo, L. W. L.; Purohit, A.; Reed, M. J.; Acharya, K. R.; Potter, B. V. L. Crystal structure of human carbonic anhydrase II at 1.95 Å resolution in complex with 667-coumate, a novel anti-cancer agent. *Biochem. J.* **2005**, *385*, 715–720.

(42) Lloyd, M. D.; Thiyagarajan, N.; Ho, Y. T.; Woo, L. W. L.; Sutcliffe, O. B.; Purohit, A.; Reed, M. J.; Acharya, K. R.; Potter, B. V. L. First crystal structures of human carbonic anhydrase II in complex with dual aromatase-steroid sulfatase inhibitors. *Biochemistry* **2005**, *44*, 6858–6866.

(43) Potterton, L.; McNicholas, S.; Krissinel, E.; Gruber, J.; Cowtan, K.; Emsley, P.; Murshudov, G. N.; Cohen, S.; Perrakis, A.; Noble, M. Developments in the CCP4 molecular-graphics project. *Acta Crystallogr., Sect. D: Biol. Crystallogr.* **2004**, *60*, 2288–2294.
(44) Persistence of Vision (TM) Raytracer; Persistence of Vision Pty. Ltd. L Williamstown, Victoria, Australia, 2004; http://www.povray.org/.
(45) The CCP4 suite: programs for protein crystallography. *Acta Crystallogr., Sect. D: Biol. Crystallogr.* **1994**, *50*, 760−763.
(46) Emsley, P.; Cowtan, K. Coot: model-building tools for molecular graphics. *Acta Crystallogr., Sect. D: Biol. Crystallogr.* **2004**, *60*, 2126–2132.
(47) Appel, R.; Berger, G. Über das Hydrazidosulfamid (On hydrazidosulfamide.). *Chem. Ber.* **1958**, *91*, 1339–1341.
(48) Armstrong, J. M. D.; Myers, D. V.; Verpoorte, J. A.; Edsall, J. T. Purification and Properties of Human Erythrocyte Carbonic Anhydrases. *J. Biol. Chem.* **1966**, *241*, 5137–5149.
(49) Otwinowski, Z.; Minor, W. Processing of X-ray diffraction data collected in oscillation mode. In *Methods Enzymol.*, Carter, C. W. J., Sweet, R. M., Eds.: Academic Press: New York, 1997; pp 307−326.
(50) McCoy, A. J.; Grosse-Kunstleve, R. W.; Adams, P. D.; Winn, M. D.; Storoni, L. C.; Read, R. J. Phaser crystallographic software. *J . Appl. Cryst.* **2007**, *40*, 658–674.
(51) Murshudov, G. N.; Vagin, A. A.; Dodson, E. J. Refinement of macromolecular structures by the maximum-likelihood method. *Acta Crystallogr., Sect. D: Biol. Crystallogr.* **1997**, *53*, 240–255.
(52) Schuttelkopf, A. W.; van Aalten, D. M. PRODRG: a tool for high-throughput crystallography of protein−ligand complexes. *Acta Crystallogr., Sect. D: Biol. Crystallogr.* **2004**, *60*, 1355–1363.